A DISSERTATION ON

Effect Of Doping On Growth And Field Emission Properties Of Spherical Carbon Nanotube (CNT) Tip Placed Over Cylindrical Surface

SUBMITTED IN PARTIAL FULFILLMENT OF THE REQUIREMENTS FOR THE AWARD OF THE DEGREE OF

MASTER OF TECHNOLOGY IN
NANOSCIENCE AND TECHNOLOGY

SUBMITTED BY

ISHA SANTOLIA

ROLLNO. 2K12/NST/07

UNDER THE SUPERVISION OF

Prof. Suresh C. Sharma

DEPARTMENT OF APPLIED PHYSICS

DELHI TECHNOLOGICAL UNIVERSITY

DELHI -110042

SESSION 2012-2013

CERTIFICATE

This is to certify that the dissertation title "***Effect of doping on growth and field emission properties of Spherical Carbon Nanotube (CNT) tip placed over cylindrical surface"*** is the authentic work of **Miss. Isha Santolia** under my guidance and supervision in the partial fulfillment of requirement towards the degree of Master of Technology in Nanoscience and Technology run by the Department of Applied Physics in ***Delhi Technological University, Delhi.***

Dr. Rinku Sharma
Co. Supervisor
Associate Professor
Delhi Technological University
Delhi

Prof. S.C. Sharma
Supervisor ,Head
Dept. Of Applied Physics,
Delhi Technological University
Delhi

DECLARATION BY THE CANDIDATE

I hereby declare that the work presented in this dissertation entitled "***Effect of doping on growth and field emission properties of Spherical Carbon Nanotube (CNT) tip placed over cylindrical surface*** "has been carried out by me under the guidance of Prof.S.C.Sharma, Head, and Dr. Rinku Sharma, Department of Applied Physics, Delhi Technological University, Delhi and hereby submitted for the partial fulfillment for the award of degree of Master of Technology in Nanoscience and Technology at Applied Physics Department, Delhi Technological University, Delhi.

I further undertake that the work embodied in this major project has not been submitted for the award of any other degree elsewhere.

Isha Santolia
2K12/NST/14
M.Tech (NST)

ACKNOWLEDGEMENT

I am indebted to my dissertation supervisor **Prof. S.C. Sharma**, Head of Department (Applied Physics), Delhi Technological University, for his gracious encouragement and very valued constructive criticism that has driven me to carry the project successfully.

I am deeply grateful to **Dr. Rinku Sharma**, Associate Professor (Applied Physics), Delhi Technological University for her support and encouragement in carrying out this project.

I wish to express my heart full thanks to **Ms. Aarti Tewari**, PhD Scholar, Delhi Technological University for her goodwill and support that helped me lot in successful completion of this project.

Isha Santolia
M.Tech (NST)
2K12/NST/14

TABLE OF CONTENTS

CHAPTER 3: RESEARCH WORK

LIST OF FIGURES

Fig. 1.7(i) Showing plasma as a part of universe

Fig. 1.7(ii) Showing concept of ionization and recombination in the formation of plasma ions

Fig.1.7(iii) Plasma measurement

Fig.1.7(iv) Langmuir Probe

Fig. 1.7(v) Showing measurement of plasma parameters by inserting Langmuir Probe

Fig.1.7(vi) Formulae showing value of I_s (saturation current) can be known from the graph as peak value. By using I_s we can calculate electron temperature (T_e) and electron density (n_e).

Fig .1.8(i) Showing CNT as hydrogen storage

Fig.1.8(ii) Showing CNT based Field Effect Transistor

Fig.2.1 Showing Growth mechanism of Carbon Nanotube

Fig. 2.2 Showing CNT fabrication through PMMA electron beam lithography

Fig.2.3(i) Showing variation of power on CNT diameter.

Fig.2.3(ii) Showing variation of temperature on CNT length.

Fig. 2.3(iii) Showing effect of variation of growth time on CNT growth.

Fig.2.3(iv) Showing effect of variation of pressure on growth of CNT

Fig.2.4(i) Illustrates the variation of the normalized radius a=a0 of a spherical CNT tip with time for different CNT number densities (i.e., n_{ct}=106 cm^3, 107 cm^3, 108 cm^3) and for other parameters as mentioned above.

Fig.2.4(ii) Shows the variation of the normalized radius a=a0 of a spherical CNT tip with time for different electron number densities and electron temperatures (e.g., n_{e0}=109 cm^3 and T_{e0}=0.3 eV, n_{e0}=1010 cm^3 and T_{e0}=0.4 eV, n_{e0} =1011 cm^3 and T_{e0}=0.5 eV).

Fig.2.4(iii) Displays the variation of the normalized a=a0 of a spherical CNT tip with time for different ion number densities and ion temperatures (e.g., n_{i0}=109 cm^3 and T_{i0}=2400 K, n_{i0} =1010cm^3 and T_{i0}=2600 K, n_{i0} =1011 cm^3 and T_{i0}=2800 K).

Fig. 2.6 (a) & (b) Showing TEM images of CNT

Fig. 2.7 (a)Comparison of CNT based display technology Vs Cathode ray tube (CRT) (b) Showing the CNT based Field emission display technology

Fig. 5.1: Shows the variation of the normalized radius r/r_0 of spherical CNT tip placed over cylindrical surface for undoped CNT using parameters ($n_{ct}=10^6\ \text{cm}^{-3}, n_{iA0}= n_{e0}= n_{iB0}=10^8\text{cm}^{-3}$

$$n_{A0}=n_{B0}=10^9\ \text{cm}^{-3}, T_{e0}=0.5\ \text{eV}, T_{i0}=2500\ \text{K},\ T_{n0}=T_{ct}=2000\ \text{K}$$

Fig.5.2: Shows the variation of the normalized radius r/r_0 of spherical CNT tip placed over cylindrical

surface for doped Nitrogen using the parameters as (n_{ct}=10^6cm^{-3}, $n_{iA0} = n_{iB0} = n_{iC0} = 10^9$ cm^{-3}, $n_{A0} = n_{B0} = n_{C0} = 10^8$ cm^{-3}, $n_{e0} = 10^9$ cm^{-3}, $T_{e0} = 1.5$eV, $T_{i0} = 2600$ K , $T_{n0} = T_{ct} = 2100$ K).

Fig5.3: Shows the variation of the normalized radius r/r_0 of spherical CNT tip placed over cylindrical surface for doped Boron using the parameters as (n_{ct}=10^6 cm^{-3} , $n_{iA0} = n_{iB0} = n_{iC0} = 10^7$ cm^{-3}, $n_{A0} = n_{B0} = n_{C0} = 10^{10}$ cm^{-3}, $n_{e0} = 10^7$ cm^{-3}, $T_{e0} = 1.3$eV, $T_{i0} = 2400$ K , $T_{n0} = T_{ct} = 1950$ K).

Fig.5.4: Shows the variation of normalized ion density for Carbon un-doped CNT (n_{iA0}) , Nitrogen doped CNT (n_{iC0}) , Boron doped CNT(n_{iC0}).The parameters taken are (n_{e0}=10^8 cm^{-3} and T_{e0}=0.5eV, n_{e0}=10^9 cm^{-3} and T_{e0}=1.5eV, n_{e0}=10^7 cm^{-3} and T_{e0}=1.3eV respectively).

Fig.5.5: Shows the field emission factor for different types of CNTs, i.e,
for Undoped CNT,N-doped CNT, B-doped CNT.

Fig.5.6: Shows the variation of field emission factor β with respect to different lengths of CNT for all three cases i.e. Undoped CNT, Boron doped CNT and Nitrogen doped CNT.

ABSTRACT

Research into Carbon Nanotube based field emission devices has made significant advances—both scientifically and technologically—during the last decade, and the first products will soon enter the market. Carbon Nanotubes as electron field emitters can be used in Field Emission Flat Panel Displays, Electron microscopes and other electron emitting devices. The efficiency and field emission capacity of the devices can be further enhanced by doping Carbon Nanotubes with hetro-atom such as Nitrogen. The effect of adding Boron on Carbon Nanotubes is also studied.

In this thesis work we have theoretically investigated the effect of doping of hetero-atoms on the growth and field emission properties of Carbon Nanotubes (CNTs) tip placed over a cylindrical surface in complex plasma. The effect of doping elements of N and B on the growth of CNTs namely the tip radius has been carried out for typical glow discharge plasma parameters. A theoretical model incorporating kinetics of plasma species such as electron, ions and neutral atoms including doping elements like nitrogen (N) and Boron (B) and energy balance of CNTs in a complex plasma has been developed.

It is found that N and B as doping elements affect the radius of CNTs extensively. We obtain small radii of CNT doped with N and large radius of CNT doped with B. The field emission characteristics from CNTs have therefore been suggested on the basis of results obtained. This calculation is done with the help of Mathematica 9.0 software.

CHAPTER 1: INTRODUCTION

1.1 Nanomaterials

Nanostructure science and technology is a broad and interdisciplinary area of research and development activity that has been growing explosively worldwide in the past few years. It has the Potential for revolutionizing the ways in which materials and products are created and the range and nature of functionalities that can be accessed. It is already having a significant commercial impact, which will assuredly increase in the future.

Nanomaterials are materials of a single unit size (in at least one dimension) between 1 and 1000 **nanometers** (10^{-9} meter) but is usually 1—100 nm. A nanometer is one millionth of a millimeter - approximately 100,000 times smaller than the diameter of a human hair. Nanomaterials are of interest because at this scale unique optical, magnetic, electrical, and other properties emerge. These emergent properties have the potential for great impacts in electronics, medicine, and other fields.

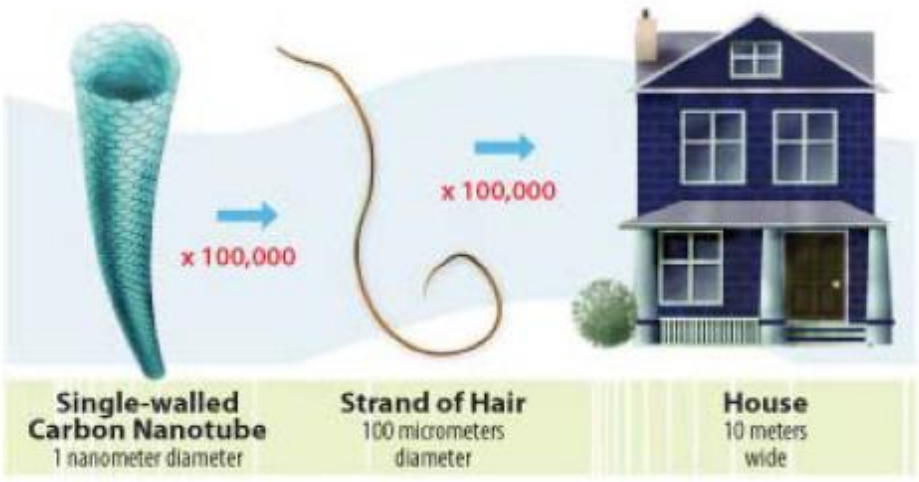

Fig. 1.1 Nanomaterial (For example: Carbon nanotube)

1.2. Classification of Nanomaterials

Nanomaterials can be nanoscale in one dimension (eg. surface films), two dimensions (eg. strands or fibres) , or three dimensions (eg. particles). They can exist in single, fused, aggregated or agglomerated forms with spherical, tubular, and irregular shapes. Common types of nanomaterials include **nanotubes, dendrimers, quantum dots and fullerenes.**

According to Siegel, Nanostructured materials are classified as ***Zero dimensional***, ***one dimensional, two***

dimensional, three dimensional nanostructures.

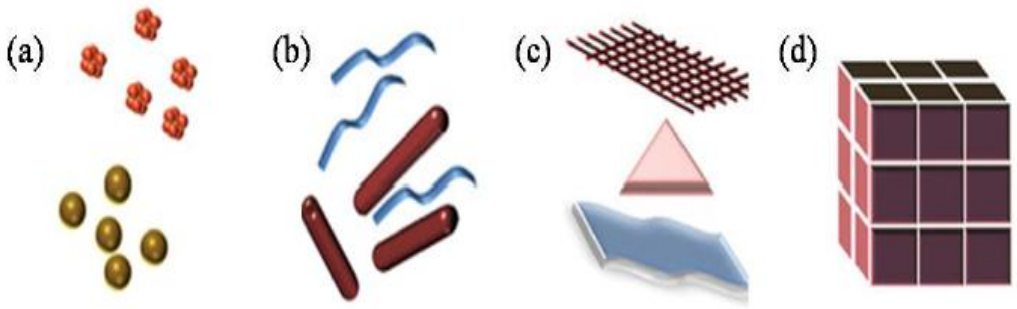

Fig. 1.2. Classification of Nanomaterials (a) 0D spheres and clusters, (b) 1D nanofibers, wires, and rods, (c) 2D films, plates, and networks, (d) 3D nanomaterials.

1.3. Nanomaterial – Generation Methods

Nanomaterials deal with very fine structures: a nanometer is a billionth of a meter. This indeed allows us to think in both the ***'bottom up' or the 'top down'*** approaches (Fig.1.3) to synthesize nanomaterials, i.e. either to assemble atoms together or to dis-assemble (break, or dissociate) bulk solids into finer pieces until they are constituted of only a few atoms. This domain is a pure example of interdisciplinary work encompassing physics, chemistry, and engineering up to medicines.

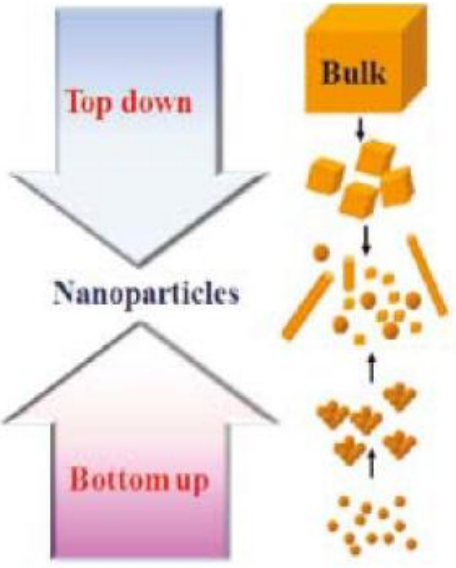

Fig.1.3 Showing Top Down and Bottom Up Approaches of Nanoparticles generation

1.4.(i) TOP DOWN APPROACH : Physical Methods

Physical methods consists of techniques as :

1) Ball Milling
2) thermal evaporation
3) lithography

Such ways of nanomaterial synthesis comes under " Top down " approach as the material is prepared not by cluster assembly but by the structural decomposition of coarser-grained structures as the result of severe plastic deformation. This has become a popular method to make nanocrystalline materials because of its simplicity, the relatively inexpensive equipment needed, and the applicability to essentially the synthesis of all classes of materials.

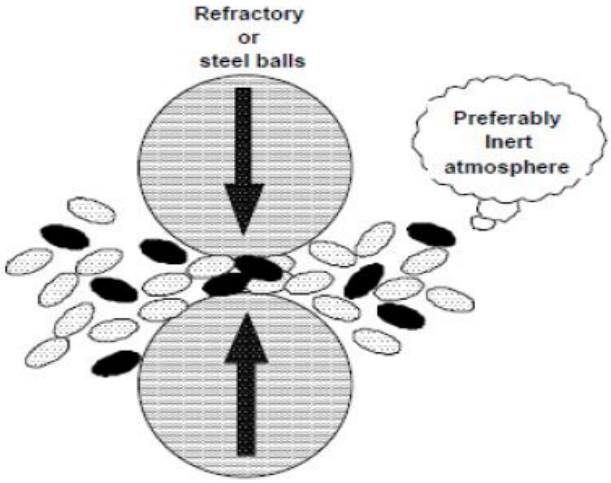

Fig. 1.4.(i) Schematic representation of the principle of mechanical milling

1.4.(ii) BOTTOM UP APPROACH: Chemical Methods

Chemical methods are "Bottom up" methods of synthesis of nanomterials. These are made by aggregation and accretion of very small particles into nanoparticles. There are several approach towards chemical synthesis root of nanofabrication. Some of the methods are listed below:

1) Self Assembly
2) Sol Gel
3) Chemical Vapor Deposition

1) Self Assembly

Self-assembly is a phenomenon where the components of a system assemble themselves spontaneously via an interaction to form a larger functional unit. This spontaneous organization can be due to direct specific interaction and/or indirectly through their environment.

It is the Selective attachment of molecules to specific surfaces on the material and the **accretion** of electrons and ions on the surface of nanoparticles.

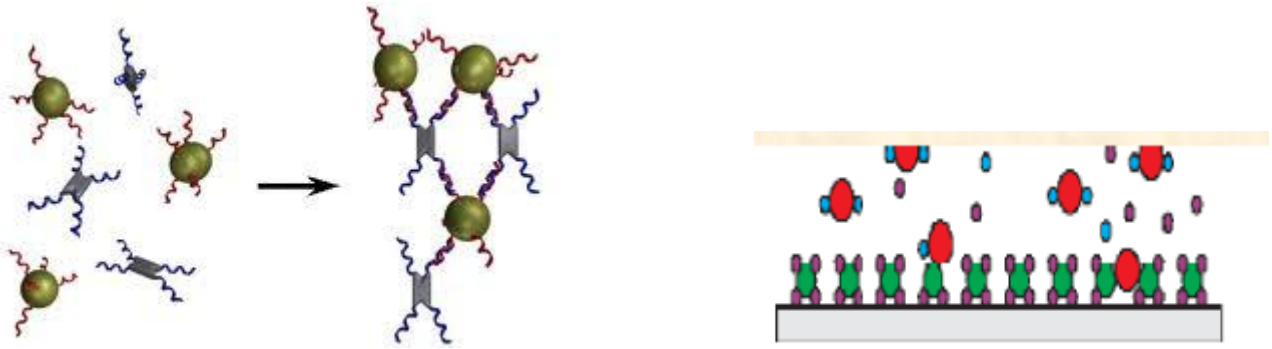

(a)

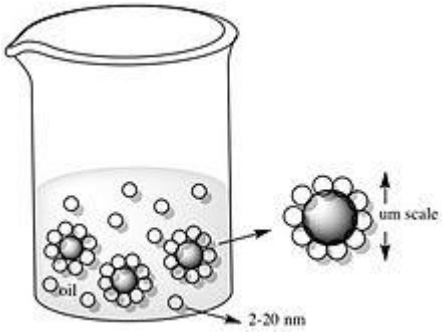

(b)

Fig.1.4.(ii) (a) Accretion of ions and molecules on the thin film surface (b) Self assembly of oil particles in water

2) Sol Gel Process

The sol-gel process, involves the evolution of inorganic networks through the formation of a colloidal suspension (sol) and gelation of the sol to form a network in a continuous liquid phase (gel). The precursors for synthesizing these colloids consist usually of a metal or metalloid element surrounded by various reactive ligands. The starting material is processed to form a dispersible oxide and forms a sol in

contact with water or dilute acid. Removal of the liquid from the sol yields the gel, and the sol/gel transition controls the particle size and shape. Calcination of the gel produces the oxide. Sol-gel method of synthesizing nanomaterials is very popular amongst chemists and is widely employed to prepare oxide materials.

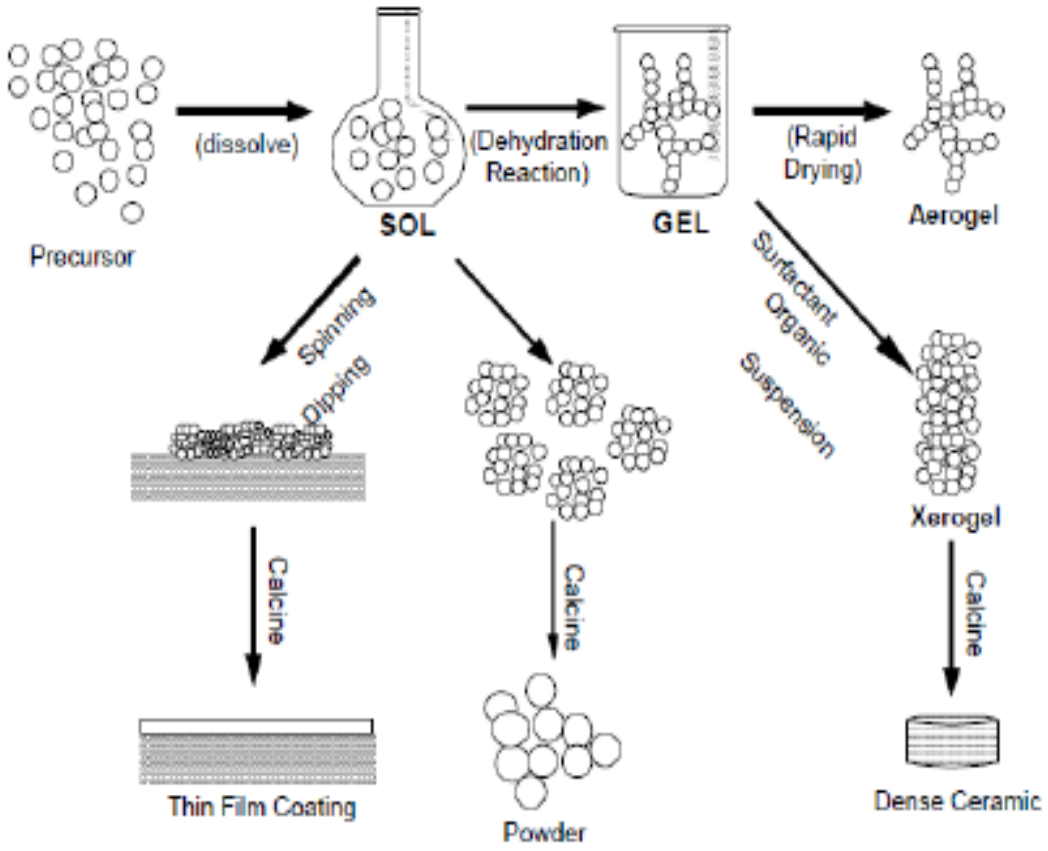

Fig.1.4.(iii) Schematic representation of sol-gel process of synthesis of nanomaterials

4) CVD : Discussed in Chapter

1.5 AN INTRODUCTION TO CARBON NANOTUBES

1.5.(i) BACKGROUND LEADING UP TO CARBON NANOTUBES

Until the mid-1980's pure solid carbon was thought to exist in only two physical forms, diamond and graphite. Diamond and graphite have different physical structures and properties however their atoms are both arranged in covalently bonded networks. These two different physical forms of carbon atoms are called allotropes.

Fig.1.5.(i)Diamond is made of carbon atoms in regular pattern of the face centered cubic Crystal.

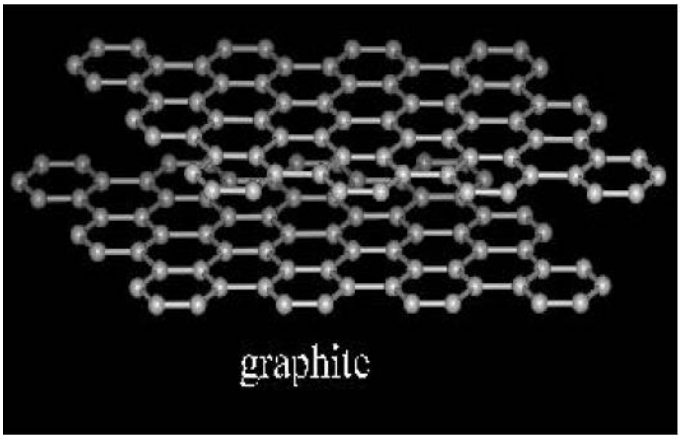

Fig.1.5.(ii) Graphite is a layered planar structure made of sheets of graphene arranged in honey comb lattice.

Another form of carbon was discovered in 1985 by a group of researchers at University of Houston and Sussex in England. They vaporized a sample of graphite with an intense pulse of laser light and used a stream of helium gas to carry the vaporized carbon into a mass spectrometer. The mass spectrum showed peaks corresponding to clusters of carbon atoms composed of 60 carbon atoms, C_{60}. It was later known as "buckminsterfullerene" or "buckyball" named after famous architect, Buckminster Fuller. This was recognized as the new allotrope of carbon.

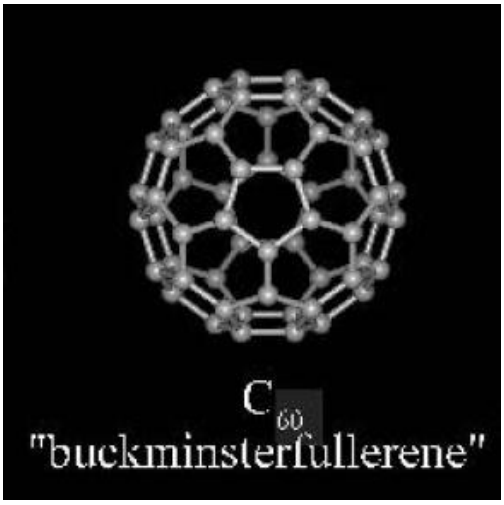

Fig.1.5.(iii) Buckminsterfullerene C_{60}

1.5.(ii) DISCOVERY OF CARBON NANOTUBES

It was also discovered that carbon atoms can form long cylindrical tubes. These tubes were originally called "buckytubes" but now are better known as **CARBON NANOTUBES (CNT)** for short. These molecules are shaped like a tube.

Carbon nanotubes have unique physical and chemical properties that chemists are trying to better understand through laboratory research. One of the physical properties of carbon nanotubes is that it's possible to make them only a single atomic layer thick.

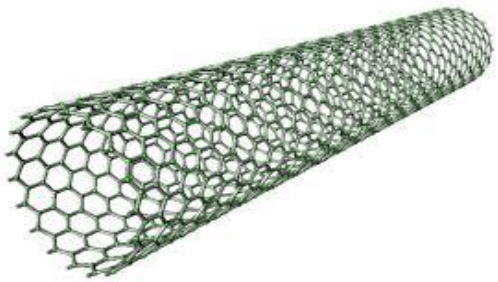

Fig.1.5.(iv) Carbon Nanotube (CNT)

A carbon nanotube (CNT) is hollow cylinder formed by rolling graphite sheets. Carbon-carbon bonding in nanotubes is sp^2. However, circular curvature of the nanotubes may cause rearrangement of σ and π bonding leading to σ – π rehybridization, in which three σ bonds are slightly out of plane. For compensation the π orbital is more delocalized outside the tube. This makes CNTs mechanically stronger, electrically and thermally more conductive and chemically and biologically more active than graphite. This also causes ***the incorporation of topological defects such as pentagons and heptagons into the hexagonal network to form capped, bend or helical tubes where electrons will be localized in pentagons and heptagons because of redistribution of π electrons.***

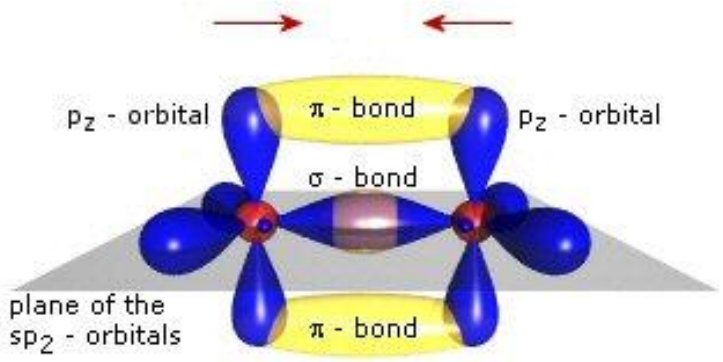

Fig.1.5.(v) Sp^2 bonding in Carbon Nanotubes

1.5.(iii) TYPES OF CNTs

Based on number of sheets rolled up, nanotubes are classified in two categories:

1) Single-Walled Nanotubes **(SWNTs)**
2) Multi-Walled Nanotubes **(MWNTs)**

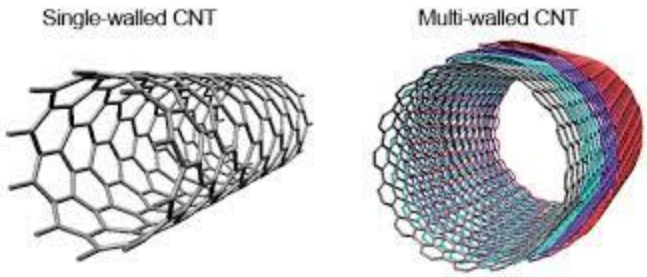

(1) (2)

Fig. 1.5.(vi) Single walled CNT and (2) Multi walled CNT

A single-walled nanotube (SWNT) is a hollow cylinder of a single graphite sheet. The inner diameter of SWNT is extremely narrow typically 1 nm. SWNTs were discovered in 1993 by arc discharge evaporation method. Generally, SWNTs produced by conventional arc-discharge method are capped and they appear in the form of bundles of tubes or ropes of tubes.

1.5.(iv) MAIN CONFIGURATIONS OF CARBON NANOTUBES

Depending upon the type of folding of carbon nanotube sheet there are three main configurations of Carbon Nanotubes namely :

1) Arm Chair
2) Zig Zag
3) Chiral

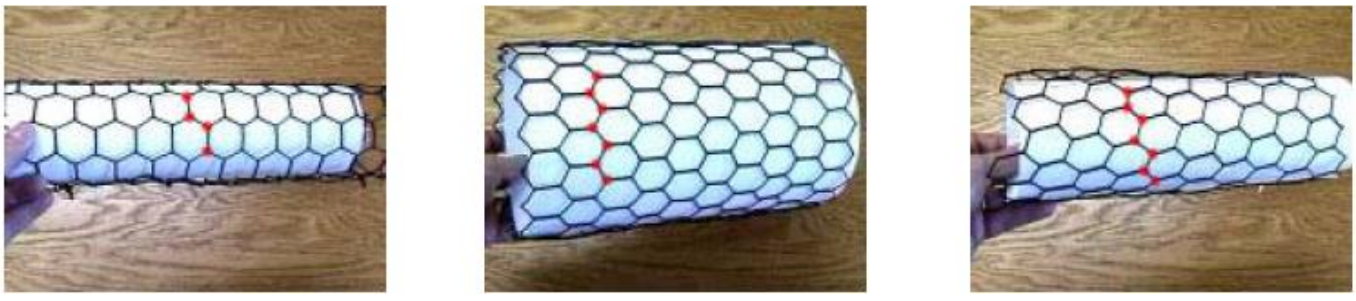

(1) (2) (3)

Fig.1.5.(vii) Showing the different configurations of CNT 1)Arm Chai 2) Zig Zag and 3) Chiral.

The way the graphene sheet is wrapped is represented by a pair of indices (*n*, *m*). The integers *n* and *m* denote the number of unit vectors along two directions in the honeycomb crystal lattice of graphene. If *m* = 0, the nanotubes are called zigzag nanotubes, and if *n* = *m*, the nanotubes are called armchair nanotubes. Otherwise, they are called chiral. The diameter of an ideal nanotube can be calculated from its (n, m) indices as follows.

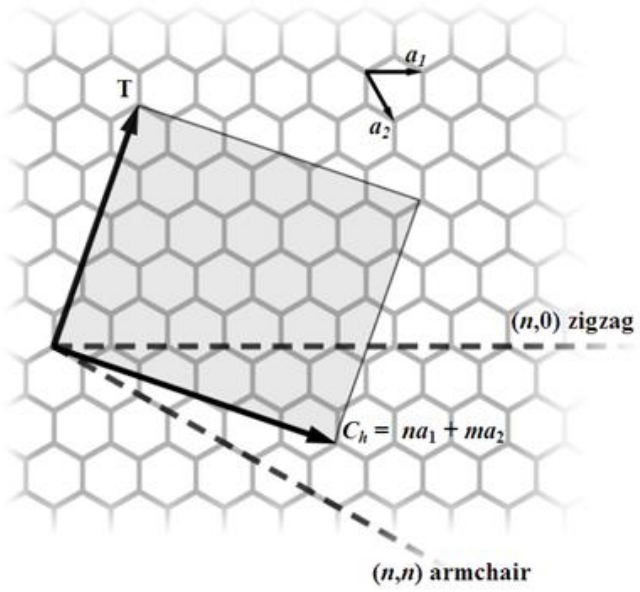

Fig.1.5.(viii) Showing the Chiral vector

$$d = \frac{a}{\pi}\sqrt{(n^2 + nm + m^2)} = 78.3\sqrt{((n+m)^2 - nm)}\text{pm}.$$

where *a* = 0.246 nm,

SWNTs are an important variety of carbon nanotube because most of their properties change significantly with the (*n*, *m*) values, and this dependence is non-monotonic. In particular, their band gap can vary from zero to about 2 eV and their electrical conductivity can show metallic or semiconducting behaviour. Single-walled nanotubes are likely candidates for miniaturizing electronics. The most basic building block of these systems is the electric wire, and SWNTs with diameters of an order of a nanometer can be excellent conductors.

1.5.(v) PROPERTIES OF CNT

Nanomaterials have the structural features in between of those of atoms and the bulk materials. While most microstructured materials have similar properties to the corresponding bulk materials, the properties of materials with nanometer dimensions are significantly different from those of atoms and bulks materials. This is mainly due to the nanometer size of the materials which render them: (i) large fraction of surface atoms; ***(ii) high surface energy; (iii) spatial confinement; (iv) reduced imperfections, which do not exist in the corresponding bulk materials.***

Carbon nanotubes features a number of extraordinary properties, amongst which are:

1) **Mechanical Strength**
2) **High Electric Conductivity**
3) **High Thermal Conductivity**
4) **Field Emission**

A brief Comparison of Properties of CNT with other materials

Table 1. Mechanical Properties of Engineering Fibers

Fiber Material	Specific Density	E (TPa)	Strenght (GPa)	Strain at Break (%)
Carbon Nanotube	1.3 – 2	1	10 – 60	10
HS Steel	7.8	0.2	4.1	< 10
Carbon Fiber – PAN	1.7 – 2	0.2 - 0.6	1.7 – 5	0.3 - 2.4
Carbon Fiber – Pitch	2 - 2.2	0.4 - 0.96	2.2 - 3.3	0.27 - 0.6
E/S – glass	2.5	0.07 / 0.08	2.4 / 4.5	4.8
Kevlar* 49	1.4	0.13	3.6 - 4.1	2.8

Table 2. Transport Properties of Conductive Materials

Material	Thermal Conductivity (W/m.k)	Electrical Conductivity
Carbon Nanotubes	> 3000	106 – 107
Copper	400	6 x 107
Carbon Fiber – Pitch	1000	2 - 8.5 x 106
Carbon Fiber – PAN	8 – 105	6.5 - 14 x 106

1) Mechanical properties

The carbon nanotubes are expected to have high stiffness and axial strength as a result of the carbon-carbon sp^2 bonding [1]. The practical application of the nanotubes requires the study of the elastic response, the inelastic behavior and buckling, yield strength and fracture. Efforts have been applied to the experimental [2–5] and theoretical [6–8,9,10], investigation of these properties. In 2000, a multi-walled carbon nanotube was tested to have a tensile strength of 63 gigapascals (GPa). Further studies, such as one conducted in 2008, revealed that individual CNT shells have strengths of up to ~100 GPa, which is in agreement with quantum/atomistic models. Since carbon nanotubes have a low density for a solid of 1.3 to 1.4 g/cm^3, its specific strength of up to 48,000 $kN \cdot m \cdot kg^{-1}$ is the best of known materials, compared to high-carbon steel's 154 $kN \cdot m \cdot kg^{-1}$.The mechanical properties of MWNTs were also measured by Wong *et al*. [3] by use of atomic force microscopy (AFM).

2) Electrical Properties:

Rolling up a graphene sheet on a nano-meter scale has dramatic consequences on the electrical properties. Because of the symmetry and unique electronic structure of graphene, the structure of a nano-tube strongly affects its electrical properties. The chirality and diameter of a CNT is extremely important, because it influences its properties. In electrical terms, chirality and diameter determine whether a CNT will behave as a metal or a semiconductor. Theoretical calculations **(Hamada *et al.* 1992; Mintmire *et al.* 1992; Saito *et al*.1992)** showed early on that the electronic properties of the CNTs are very sensitive to their geometric structure. Although graphene is a zero-gap semiconductor, theory has predicted that the CNTs can be metals or semiconductors with different sized energy gaps, depending very sensitively on the diameter and helicity of the tubes, i.e. on the indices (n, m). It is due to the unique band structure of a graphene sheet, which has states crossing the Fermi level at only two in equivalent points in k-space, and to the quantization of the electron wave vector along the circumferential direction. An isolated sheet of graphite is a zero-gap semiconductor whose electronic structure near the Fermi energy is given by an occupied π band and an empty $\pi*$ band. These two bands have linear dispersion and, as shown in figure 2, meet at the Fermi level at the K point in the Brillouin zone. The Fermi surface of an ideal graphite sheet consists of the six corner K points. When forming a tube, owing to the periodic boundary conditions imposed in the circumferential direction, only a certain set of k states of the planar graphite sheet is allowed. The allowed set of k values, indicated by the lines in figure 1.5.(viii), depends on the diameter and helicity of the tube. Whenever the allowed k include the point K, the system is a metal with a non-zero density of states at the Fermi level, resulting in a 1D metal with two linear dispersing bands. When

the point K is not included, the system is a semiconductor with different sized energy gaps. It is important to note that the states near the Fermi energy in both the metallic and the semiconducting tubes are all from states near the K point, and hence their transport and other electronic properties are related to the properties of the states on the allowed lines.

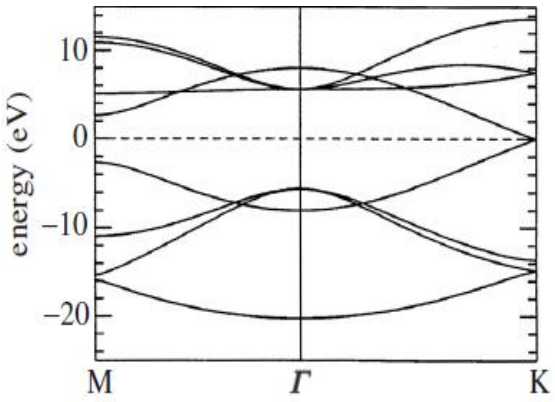

Fig .1.5.(viii) Showing tight band graph of CNT

3) Thermal Properties:

The thermal properties of CNTs display a wide range of behaviors which stem from both their relation to a 2D graphene layer and their unique structure and tiny size. The specific heat of individual nanotubes should be similar to that of 2D graphene at high temperatures, with the effects of phonon quantization becoming apparent at lower temperatures for SWNTs of small diameter (less than 2 nm). The specific heat *C* of CNTs is dominated by the phonon contribution (C_{ph}). At low temperature both the quantized phonon structure and the stiffening of the acoustic modes will cause the specific heat of carbon nanotube to have enhanced thermal properties than that of other materials like graphite etc.

4) Field Emission: Discussed in Chapter 2

1.5.(vi) SYNTHESIS OF CARBON NANOTUBES

The MWNTs were first discovered in the soot of the arc-discharge method by Iijima [11]. This method has been used long before that in the production of carbon fibers and fullerenes. It took 2 years to Iijima and Ichihashi [12], and Bethune et al. [13] to synthesize SWNTs by use of metal catalysts in the arc-discharge method in 1993. A significant progress was achieved by laser-ablation synthesis of bundles of

aligned SWNTs with small diameter distribution by Smalley and co-workers [14]. Catalytic growth of nanotubes by the chemical vapor decomposition (CVD) method was first used by Yacaman et al. [15]. The industrial application of the carbon nanotubes requires the development of techniques for large-scale production of defect-free nanotubes. In this section, the major progress in the nanotube production methods will be outlined . There are basically three main production techniques :

1) ARC DISCHARGE

In 1991, Iijima reported the preparation of a new type of finite carbon structures consisting of needle-like tubes[11]. The tubes were produced using an arc-discharge evaporation method similar to that used for the fullerene synthesis. The carbon needles, ranging from 4 to 30 nm in diameter and up to 1 mm in length, were grown on the negative end of the carbon electrode used for the direct current (dc) arc-discharge evaporation of carbon in an argon-filled vessel (100 Torr) (see Fig. 1.5.(ix)).

On each of the tubes the carbon-atom hexagons were arranged in a helical fashion about the needle axis. The helical pitch varied from needle to needle and from tube to tube within a single needle. The tips of the needles were usually closed by curved, polygonal, or cone-shaped caps.

In this process, the carbon contained in the negative electrode sublimates because of the high-discharge temperatures. Because nanotubes were initially discovered using this technique, it has been the most widely used method of nanotube synthesis. The yield for this method is up to 30% by weight and it produces both single- and multi-walled nanotubes with lengths of up to 50 micrometers with few structural defects.

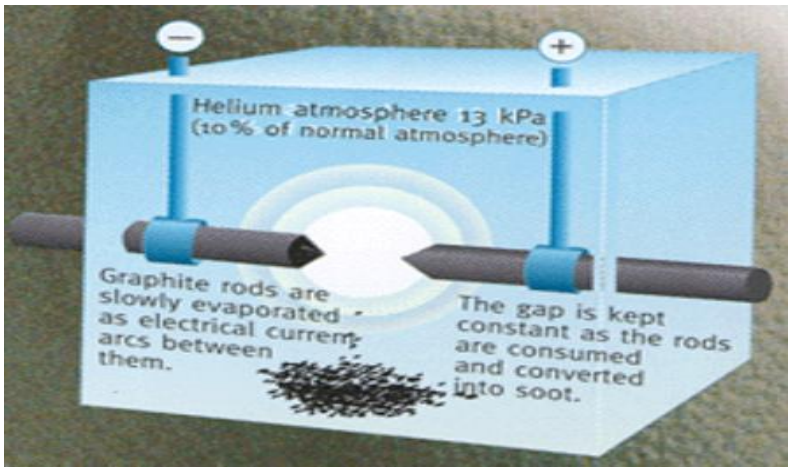

Fig. 1.5.(ix) Showing ARC Discharge method of CNT production

2) LASER ABLATION

In laser ablation, a pulsed laser vaporizes a graphite target in a high-temperature reactor while an inert gas is bled into the chamber. Nanotubes develop on the cooler surfaces of the reactor as the vaporized carbon condenses. A water-cooled surface may be included in the system to collect the nanotubes.
This process was developed by ***Dr. Richard Smalley*** and co-workers at Rice University, who at the time of the discovery of carbon nanotubes, were blasting metals with a laser to produce various metal molecules. When they heard of the existence of nanotubes they replaced the metals with graphite to create multi-walled carbon nanotubes. Later that year the team used a composite of graphite and metal catalyst particles (the best yield was from a cobalt and nickel mixture) to synthesize single-walled carbon nanotubes.

The laser ablation method yields around 70% and produces primarily single-walled carbon nanotubes with a controllable diameter determined by the reaction temperature. However, it is more expensive than either arc discharge or chemical vapor deposition.
The properties of CNTs prepared by the laser ablation method are strongly dependent on the laser properties (energy fluence, peak power, repetition rate and oscillation wavelength), the structural and chemical composition of the target material, the chamber pressure and the chemical composition, the substrate and ambient temperature and the distance between the target and the substrates.

Laser ablation, is one of the superior methods to grow SWNTs with high-quality and high-purity. In this method, which was first demonstrated by Smalley's group in 1995,[16] the principles and mechanisms are similar to the arc discharge with the difference that the energy is provided by a laser hitting a graphite pellet containing catalyst materials (usually nickel or cobalt)[17]. Almost all the lasers used for the ablation have been Nd: YAG and CO2. For example, Zhang et al. prepared SWNTs by continuous wave CO2 laser ablation without applying additional heat to the target. They observed that the average diameter of SWNTs produced by CO2 laser increased with increasing laser power.[18]–[20]

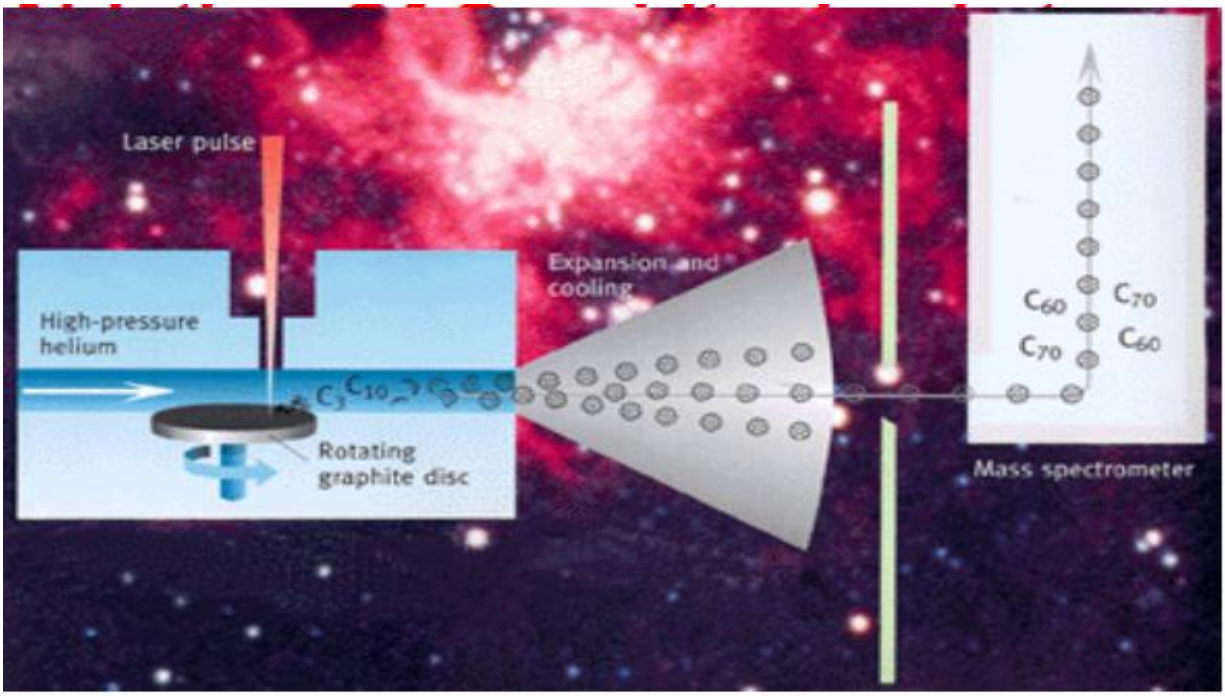

Fig. 1.5.(x) Showing Laser Ablation method of synthesis of CNT

3) CHEMICAL VAPOUR DEPOSITION

The catalytic vapor phase deposition of carbon was reported in 1952 and 1959, but it was not until 1993 that carbon nanotubes were formed by this process. In 2007, researchers at the University of Cincinnati (UC) developed a process to grow aligned carbon nanotube arrays of 18 mm length on a FirstNano ET3000 carbon nanotube growth system.

During CVD, a substrate is prepared with a layer of metal catalyst particles, most commonly nickel, cobalt, iron, or a combination. The metal nanoparticles can also be produced by other ways, including reduction of oxides or oxides solid solutions. The diameters of the nanotubes that are to be grown are related to the size of the metal particles. This can be controlled by patterned (or masked) deposition of the metal, annealing, or by plasma etching of a metal layer. The substrate is heated to approximately 700°CTo initiate the growth of nanotubes, two gases are bled into the reactor: a process gas (such as ammonia, nitrogen or hydrogen) and a carbon-containing gas (such as acetylene, ethylene, ethanol or methane). Nanotubes grow at the sites of the metal catalyst; the carbon-containing gas is broken apart at the surface of the catalyst particle, and the carbon is transported to the edges of the particle, where it forms the nanotubes. This mechanism is still being studied. The catalyst particles can stay at the tips of the growing nanotube during growth, or remain at the nanotube base,

depending on the adhesion between the catalyst particle and the substrate. Thermal catalytic decomposition of hydrocarbon has become an active area of research and can be a promising route for the bulk production of CNTs. Fluidised bed reactor is the most widely used reactor for CNT preparation. Scale-up of the reactor is the major challenge.

CVD is a common method for the commercial production of carbon nanotubes. For this purpose, the metal nanoparticles are mixed with a catalyst support such as MgO or Al_2O_3 to increase the surface area for higher yield of the catalytic reaction of the carbon feedstock with the metal particles.

Catalytic chemical vapour deposition (CCVD)—either thermal[21] or plasma enhanced (PE)—is now the standard method for the CNTs production. Moreover, there are trends to use other CVD techniques, like water assisted CVD,[22]–[24] oxygen assisted CVD,[25] hot-filament (HFCVD),[26,27] microwave plasma (MPECVD)[28],[29] or radiofrequency CVD (RF-CVD).[30] CCVD is considered to be an economically viable process for large scale and quite pure CNTs production compared with laser ablation. The main advantages of CVD are easy control of the reaction course and high purity of the obtained material, etc.[31].The function of catalyst in the CVD process is the decomposition of carbon source via either plasma irradiation (plasma-enhanced CVD, PECVD) or heat (thermal CVD) and its new nucleation to form CNTs. The most frequently used catalysts are transition metals , primary Fe, Co or Ni.

Lyu et al. produced high-quality and high-purity DWNTs b catalytic decomposition of benzene as an ideal carbon source and Fe–Mo/Al2O3 as a catalyst at 900 C. They obtained DWNTs bundles free of amorphous carbon covering on the surface and of a low defect level in the atomic carbon structure.[32]

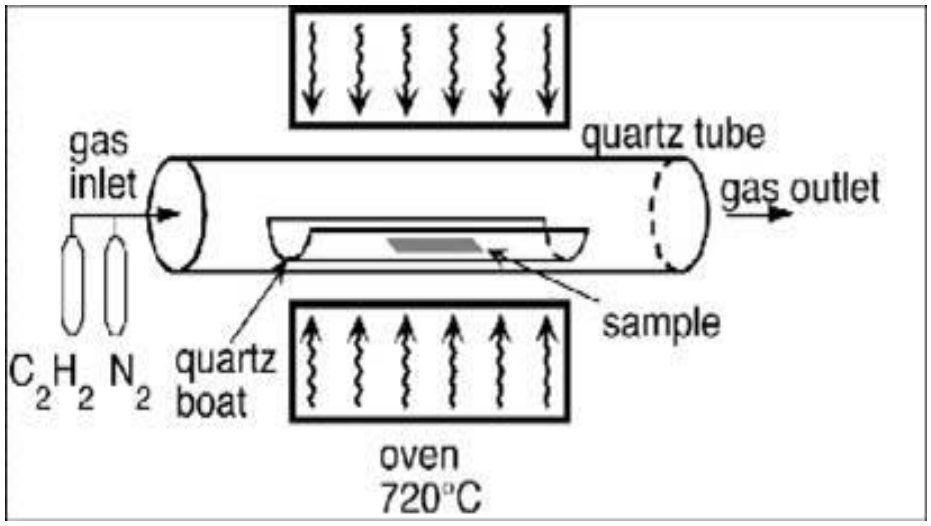

Fig. 1.5.(xi) Chemical Vapor Deposition method of preparation of Cabon Nanotubes

1.6 PLASMA ENHANCED CHEMICAL VAPOR DEPOSITION (PECVD)

Plasma-enhanced chemical vapor deposition (**PECVD**) is a process used to deposit thin films from a gas state (vapor) to a solid state on a substrate. Chemical reactions are involved in the process, which occur after creation of a plasma of the reacting gases. The plasma is generally created by RF (AC) frequency or DC discharge between two electrodes, the space between which is filled with the reacting gases. A simple direct-current (DC) discharge can be readily created at a few torr between two conductive electrodes, and may be suitable for deposition of conductive materials. However, insulating films will quickly extinguish this discharge as they are deposited. It is more common to excite a capacitive discharge by applying an alternating-current (AC) or radio-frequency (RF) signal between an electrode and the conductive walls of a reactor chamber, Frequencies of a few tens of Hz to a few thousand Hz will produce time-varying plasmas that are repeatedly initiated and extinguished; frequencies of tens of kilohertz to tens of megahertz result in reasonably time-independent discharges.

PECVD IS

- **CVD process that uses PLASMA**
- **Uses cold plasma**
- **Keeps wafers at low temperature**
- **Enhances properties of layers being Deposited**

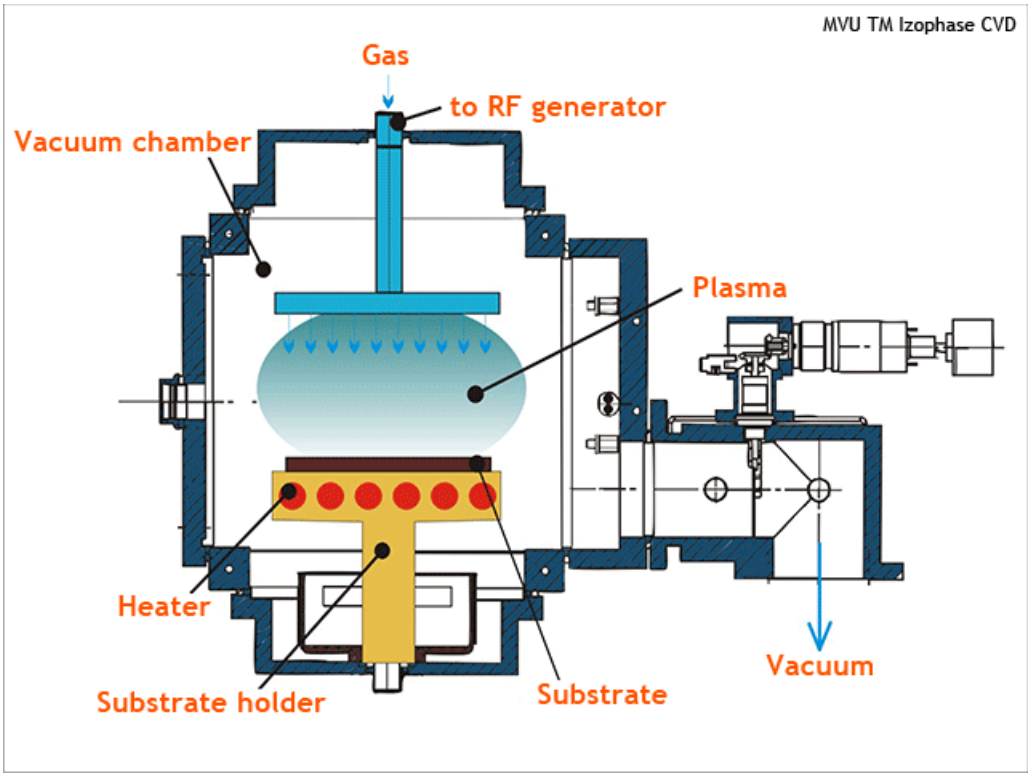

Fig. 1.6 Schematic diagram of PECVD

ADVANTAGES OF USING PECVD

- **Low operation temperature**
- **Lower chances of cracking deposited layer**
- **Good dielectric properties of deposited layer**
- **Good step coverage**
- **Less temperature dependent**
- **PECVD is not a replacement for CVD**
- **PECVD can give better layer quality than CVD**
- **PECVD has a wide variety applications**
- **PECVD is a synthesis technique which allows to make vertically aligned CNTs.**
- **Allows control of growth parameters to influence growth rate and diameter.**

DISADVANTAGES OF USING PECVD

- **Toxic by products**
- **High cost of equipment**

1.7 WHAT IS PLASMA?

Plasma is one of the four fundamental states of matter (the others being solid, liquid, and gas). It comprises the major component of the Sun. Heating a gas may ionize its molecules or atoms (reducing or increasing the number of electrons in them), thus turning it into a plasma, which contains charged particles: positive ions and negative electrons or ions. Ionization can be induced by other means, such as strong electromagnetic field applied with a laser or microwave generator, and is accompanied by the dissociation of molecular bonds, if present.

Plasma is loosely described as an electrically neutral medium of positive and negative particles (i.e. the overall charge of a plasma is roughly zero).

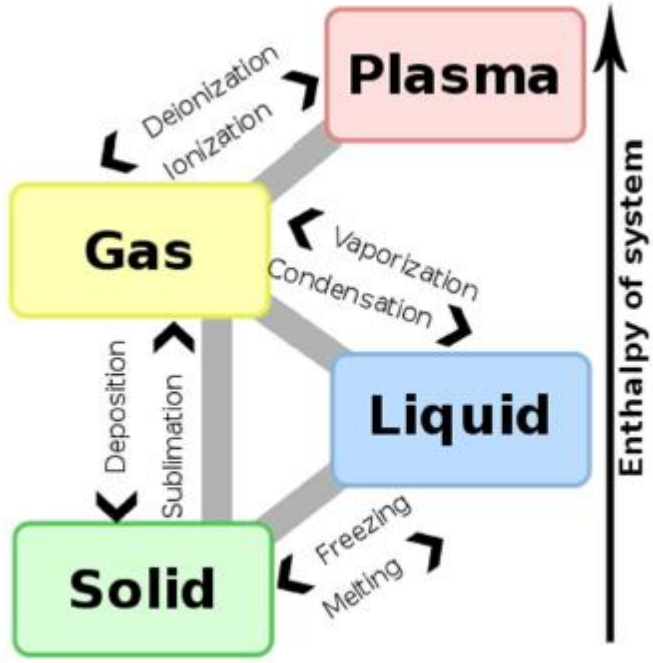

Fig.1.7 Fourth state of matter: solid - liquid - gas - plasma

It is sometimes remarked that 95% (or 99%) of the baryonic content of the universe consists of plasma.Nevertheless, it is worth pointing out the prevalence of the plasma state. In earlier epochs of the universe, everything was plasma. In the present epoch , stars, nebulae, and even interstellar space are filled with plasma. The solar system is alo permeated by plasma trapped within its magnetic field.

Terrestial plasmas are also not hard to find. They occur in lightning , fluorescent lamps, a variety of laboratory experiments, and a growing array of industrial processes. In fact, the glow discharge has recently become the mainstay of the micro-circuit fabrication industry.

Liquid and even solid- state systems can ocassionally display the collective electromagnetic effects that characerize plasma, e.g. liquid mercury exhibits many dynamical modes, such as Alfven waves, which occur in conventional plasmas.

Fig. 1.7.(i) Showing plasma as a part of universe

1.7.(i) Plasma Production Techniques:

1) Heating

2) Ionization

1.7.(ii) Basic Parameters

A plasma is a gas in which an important fraction of the atoms is *ionized*, so that the electrons and ions are separately free. When does this ionization occur? When the temperature is hot enough. Balance between collisional ionization and recombination:

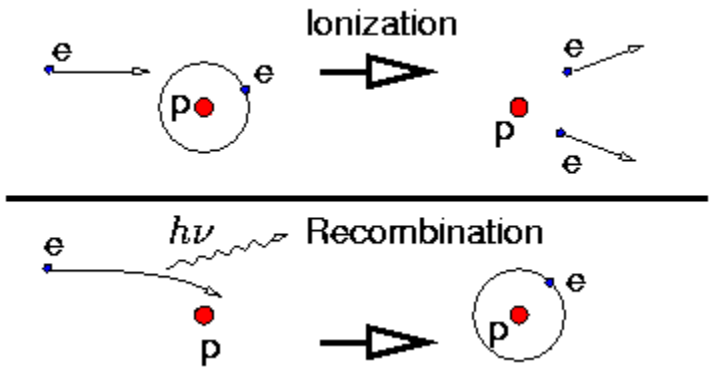

Fig. 1.7.(ii) Showing concept of ionization and recombination in the formation of plasma ions

Consider an idealized plasma consisting of an equal number of electrons, with mass m_e and charge $-e$ (here, e denotes the *magnitude* of the electron charge), and ions, with mass m_i and charge $+e$. We do not necessarily demand that the system has attained thermal equilibrium, but nevertheless use the symbol

$$T_s \equiv \frac{1}{3} m_s \langle v_s^2 \rangle$$

to denote a ***kinetic temperature/electron temperature /plasma temperature*** measured in energy units (*i.e.*, joules). Here, v is a particle speed, and the angular brackets denote an ensemble average. The kinetic temperature of species s is essentially the average kinetic energy of particles of this species. In plasma physics, kinetic temperature is invariably measured in *electron-volts* (1 joule is equivalent to 6.24×10^{18} **eV).**

Quasi-neutrality demands that

$$n_i \simeq n_e \equiv n,$$

where n_s is the number density/plasma density (*i.e.*, the number of particles per cubic meter) of species s.

Plasma Frequency

Since plasma has both positive and negative charges, they are constantly oscillating back and forth. This results in a characteristic frequency called the Plasma Frequency .The plasma frequency is a resonant frequency of the ionized gas - it depends on the square root of the electron density.

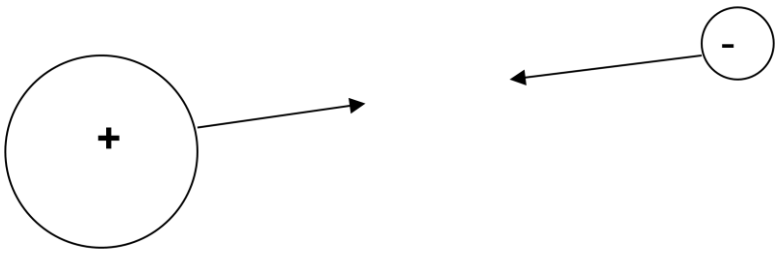

The *plasma frequency*,

$$\omega_p^2 = \frac{n e^2}{\epsilon_0 m},$$

ω_p corresponds to the typical electrostatic oscillation frequency of a given species in response to a small charge separation.

Plasma potential

The potential as it exists on average in the space between charged particles, independent of the question of how it can be measured, is called the "plasma potential", or the "space potential". If an electrode is inserted into a plasma, its potential will generally lie considerably below the plasma potential due to what is termed a *Debye sheath*. The good electrical conductivity of plasmas makes their electric fields very small. This results in the important concept of "quasi-neutrality", which says the density of negative charges is approximately equal to the density of positive charges over large volumes of the plasma ($n_e = \langle Z \rangle n_i$), but on the scale of the Debye length there can be charge imbalance. In the special case that *double layers* are formed, the charge separation can extend some tens of Debye lengths.

1.7.(iii) PLASMA MEASUREMENTS

Plasma parameters such as electron temperature, electron dendity/plasma density and plasma potential is measured by an instrument known as **langmuir probe.**

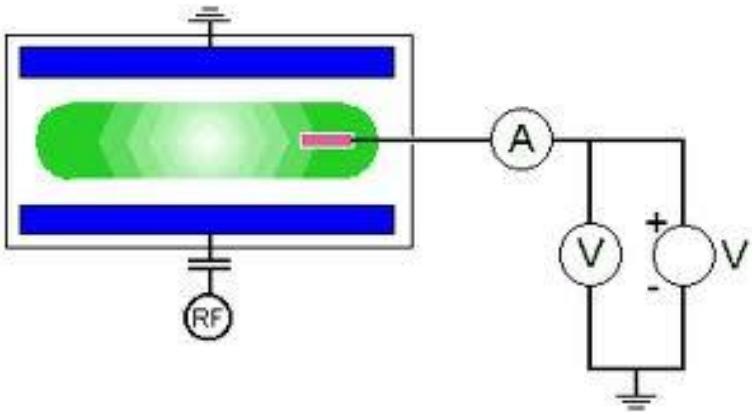

Fig.1.7.(iii) Plasma measurement

Fig.1.7.(iv) Langmuir Probe

1.7.(iv) STEPS OF PLASMA MEASUREMENT

- A Langmuir probe is inserted into the plasma and is given biased voltage with respect to a reference electrode to collect electron and positive ion currents.
- Ammeter and voltmeter connected to take the measured values of the probe.
- When no bias applied, the potential measured at tip is *floating potential (Vf)* which is less than the actual *plasma potential (Vp).*At floating potential ,an equal flow of electrons and ions causes zero net current.
- If the probe is given bias ,then potential difference is created in the plasma which creates a net flow of current .
- The measured quantities are generally plotted as the I/ V graph.

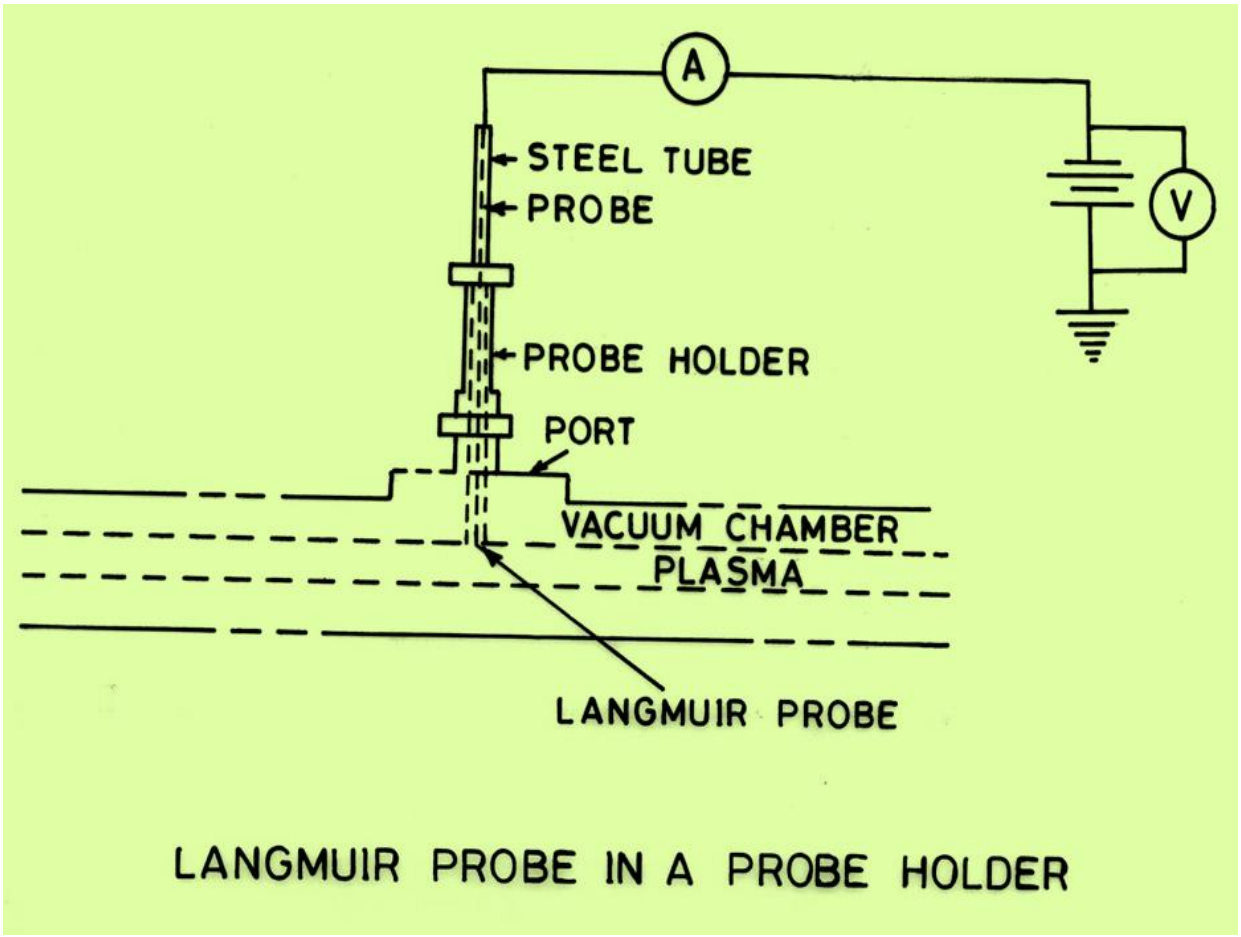

Fig. 1.7.(v) Showing measurement of plasma parameters by inserting Langmuir Probe

1.7.(v) I/V CHARACTERISTICS OF MEASURED QUANTITIES

The I/V characteristics would help us to find the values of electron temperature (T_e) and number density of plasma (n_e) from the graph as shown:

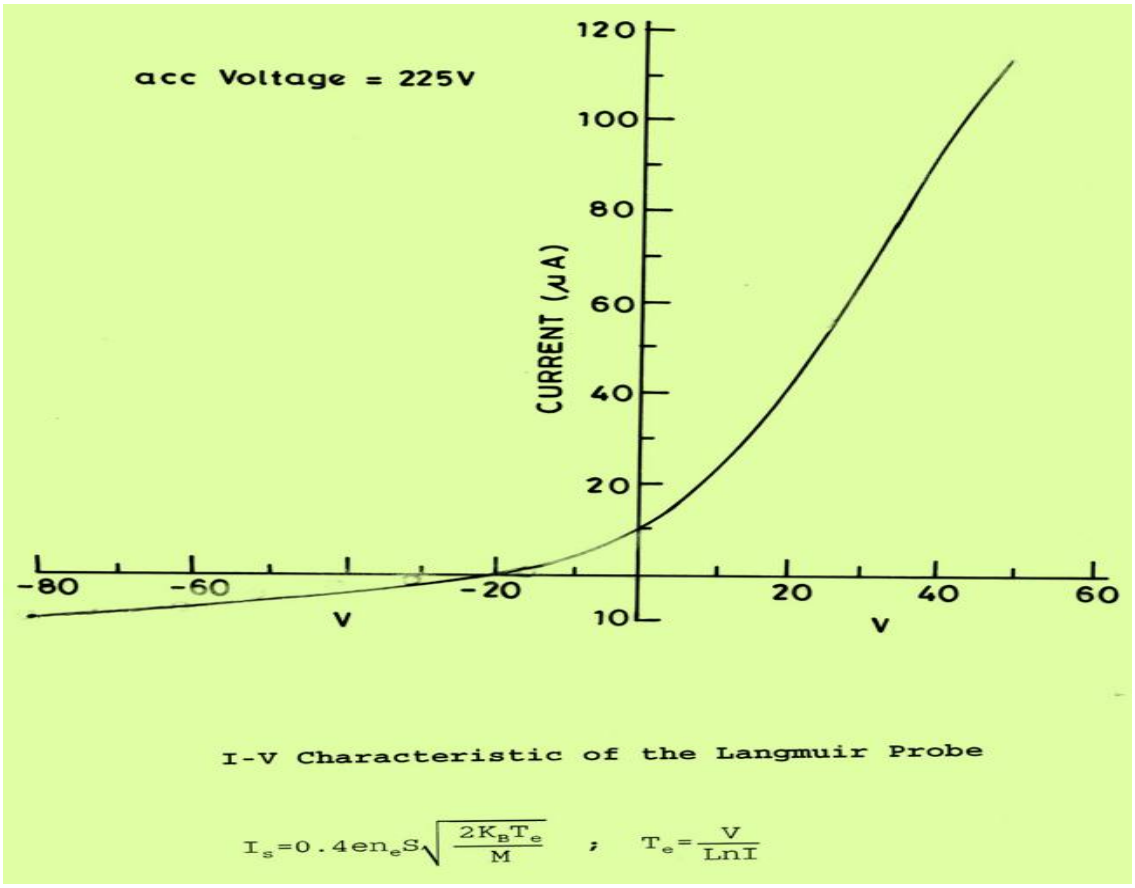

Fig.1.7.(vi) formulae showing value of I_s (saturation current) can be known from the graph as peak value. By using I_s we can calculate electron temperature (T_e) and electron density (n_e).

1.8 CNT APPLICATIONS

1) Use of carbon nanotubes in HYDROGEN STORAGE

With the accelerating demand for cleaner and more efficient energy sources, hydrogen research has attracted more attention in the scientific community. The focus of some of the research has been the development of hydrogen fuel cells, electrochemical devices that are able power buildings, cars and portable electric devices.

Hydrogen is an ideal fuel; it is abundant, renewable and its combustion produces only water vapor and heat. Until now, full implementation of a hydrogen-based energy system has been hindered in part by the challenge of storing hydrogen gas, especially onboard an automobile. New techniques being researched mahydrogen storage more compact, safe and efficient.

These new methods use carbon as a storage medium and bring us a step closer to the widespread use of hydrogen as a fuel source. Some scientists are using various approaches to shape carbon into microscopic cylindrical structures known as Nanotubes. One of the critical factors in Nanotubes' usefulness as a hydrogen storage medium is the ratio of stored hydrogen to carbon. According to the US Department of Energy, a carbon material needs to store 6.5% of its own weight in hydrogen to make fuel cells practical in cars. Such fuel cell cars could then travel 300 miles between refuelling stops.

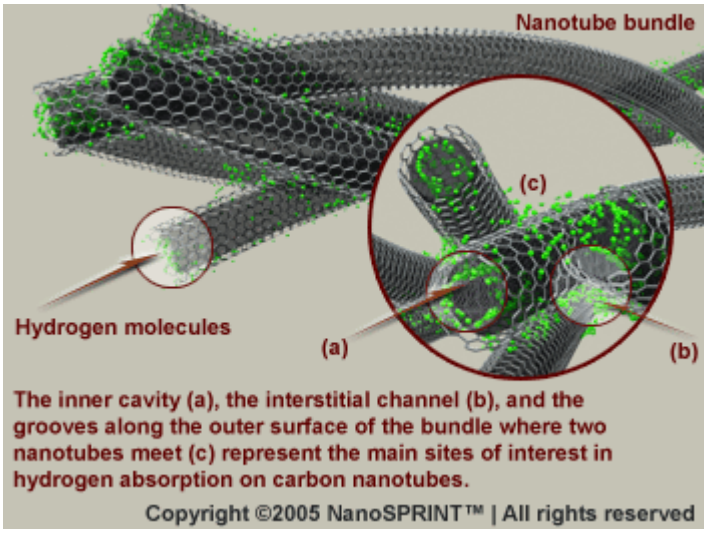

Fig .1.8.(i) Showing CNT as hydrogen storage

2) CNT based FET

Nanotube-based transistors, also known as carbon nanotube field-effect transistors (CNTFETs), can operate at room temperature and are capable of digital switching using a single electron.

A carbon nanotube field-effect transistor (CNTFET) refers to a field-effect transistor that utilizes a single carbon nanotube or an array of carbon nanotubes as the channel material instead of bulk silicon in the traditional MOSFET structure. The scaling down of devices has faced serious limits related to fabrication technology. The limits involve electron tunneling through short channels and thin insulator films, the associated leakage currents, passive power dissipation, short channel effects, and variations in device structure and doping.

These limits can be overcome to some extent and facilitate further scaling down of device dimensions by modifying the channel material in the traditional bulk MOSFET structure with a single carbon nanotube or an array of carbon nanotubes.

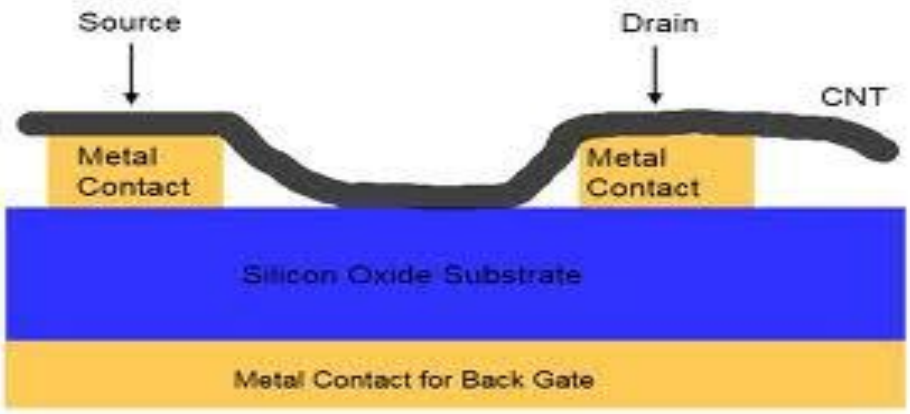

Fig.1.8.(ii) Showing CNT based Field Effect Transistor

CHAPTER 2 : LITERATURE REVIEW

2.1 Introduction

In this chapter we would see the various works and contributions of different authors in the field of Carbon Nanotube (CNT) growth process, various factors affecting its growth, influence of plasma parameters on CNT, field emission properties of Carbon Nanotubes etc.

We would see how these several factors affecting the properties of Carbon Nanotubes will help us in developing new models of growth and by using their results we can bring changes and improve upon the current characteristics like Field emission etc.

In sec. 1 we will study about the growth mechanism of Carbon nanotubes and in sec. 2 about the various factors which affect CNT growth and later on in sec. 3 about the plasma parameters which affect CNT growth and properties.

2.2 CNT Growth Mechanism

THERE ARE TWO CASES:

1)TIP GROWTH MODEL:- when the catalyst- substrate interaction is weak, hydrocarbon decomposes on the top surface of the metal, carbon diffuses down through the metal and CNT precipitates out across the metal bottom, pushing the whole metal particle off the substrate. As long as the metal top is open for fresh hydrocarbon decomposition,cnt continues to grow longer and longer. Once the metal is fully covered with excess carbon, its catalytic activity ceases and the CNT growth is stopped.

2)**BASE GROWTH MODEL:** When the catalyst substrate interaction is strong, initial hydrocarbon decomposition and carbon diffusion takes place but the cnt precipitation fails to push the metal particle up. Carbon crystallises out as a hemispherical dome. hydrocarbon deposition takes place on the lower peripheral surface of the metal. Thus CNT grows up with the catalyst particle rooted on its base.

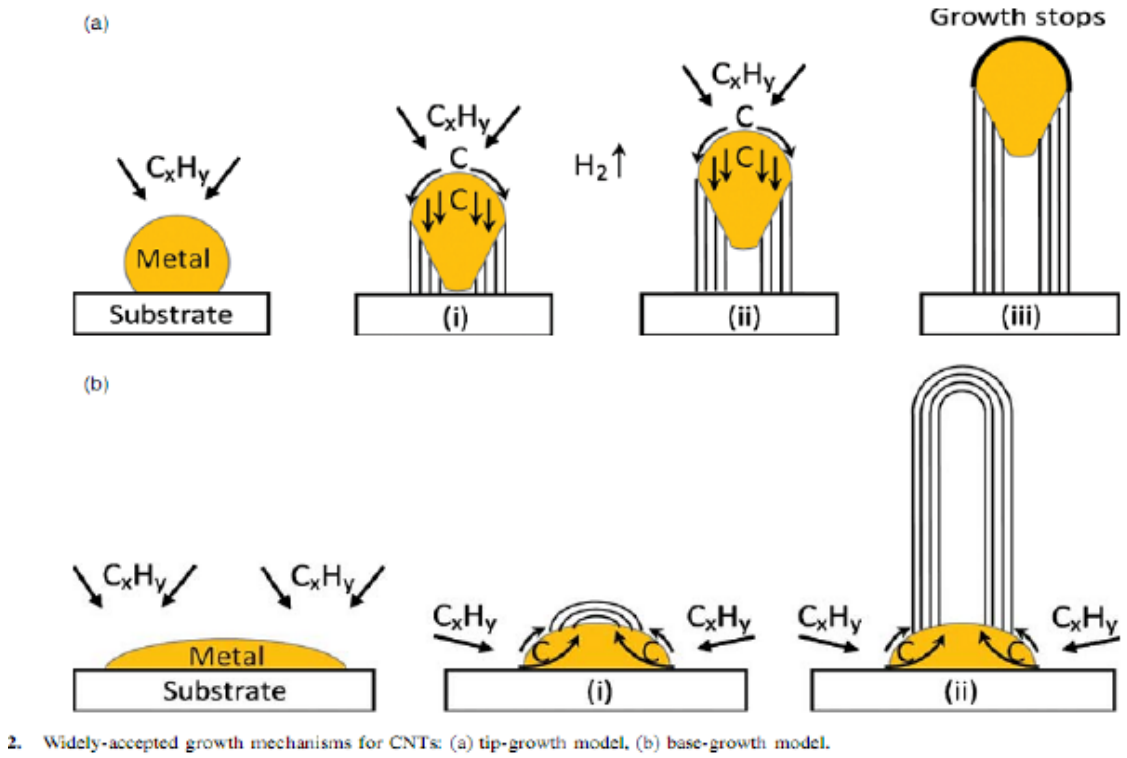

2. Widely-accepted growth mechanisms for CNTs: (a) tip-growth model, (b) base-growth model.

Fig.2.1 Showing Growth mechanism of Carbon Nanotube

2.3 Study of various factors affecting CNT growth(R.Loffler *et al.* CARBON 49 (2011) 4197 –4203)

Though there are several methods to produce carbon nanotube but to produce vertically aligned CNTs ,PECVD growth of method is generally utilised. **R.Loffler *et al.***[33] have studied the growth of vertically aligned carbon nanotubes (CNTs) from individual nickel catalyst dots , aiming at the fabrication of CNT field emitters. It was found that the growth of individual CNTs differs from that of CNT forests grown from unpatterned catalyst films, an effect that can be attributed to the difference in catalyst volumes. They further investigated some of the parameters like temperature, growth time, volume, pressure and power which influences the growth of carbon nanotube.

CNTs are grown on an oxidized silicon wafer as substrate, as depicted in Fig. 1. 100 nm of spin-coated PMMA is exposed in an electron beam lithography system after development a 7 nm Ni, which is the preferred catalyst for achieving good vertical alignment , is sputtered on and lifted off using acetone. The nickel dots have diameters of the order of 100 nm. In the PECVD process the sample is heated up to the desired growth temperature. During heating in an ammonia gas flow, the thin nickel catalyst films agglomerate .Size and volume of these droplets are determined by the available catalyst volume.

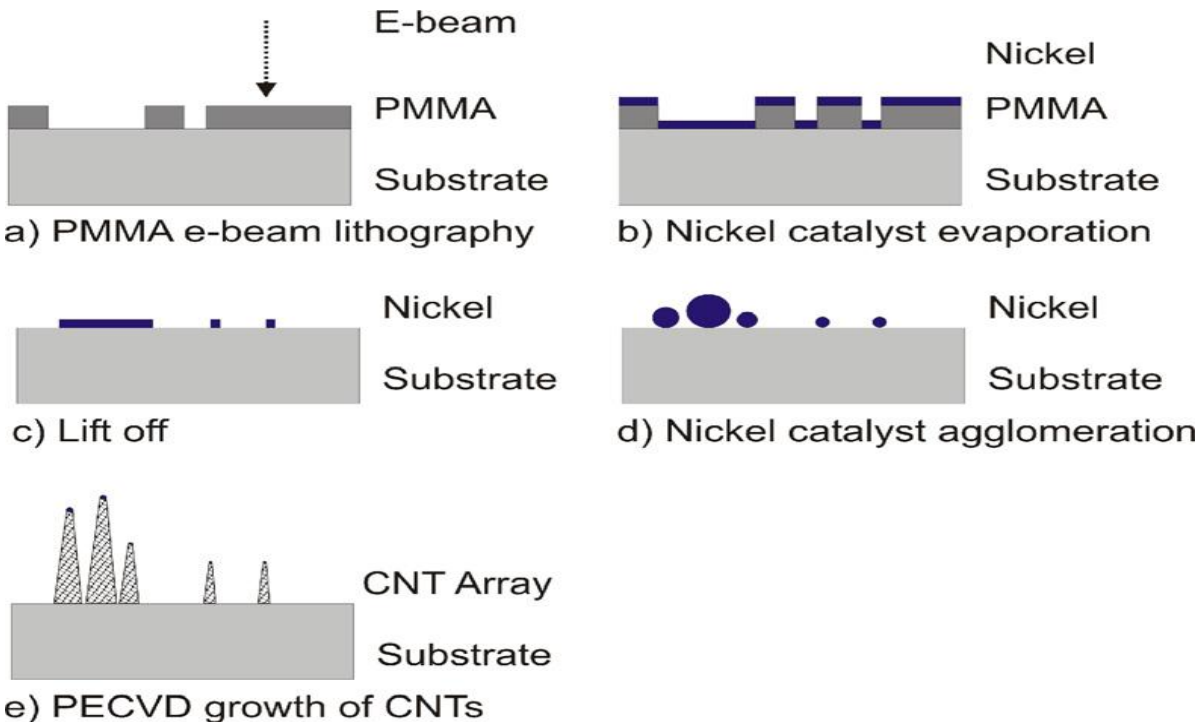

Fig. 2.2 Showing CNT fabrication through PMMA electron beam lithography

2.3.(i) Systematic variation of PECVD parameters

Systematic investigation of the influence of the key growth parameters on the growth of single vertical CNTs was done, all process parameters were kept constant, while one parameter was varied at a time. PECVD process parameters were taken as 600ºC substrate temperature, 10W plasma power, 4.3 mbar process gas pressure and 10 min growth time .

1) Variation of power

Increased power results in a greater electric field within the plasma sheath. Also the etch rate increases due to strong ion bombardment. The catalytic particle is sputtered during the PECVD process so that the diameter of the CNT decreases during the process.

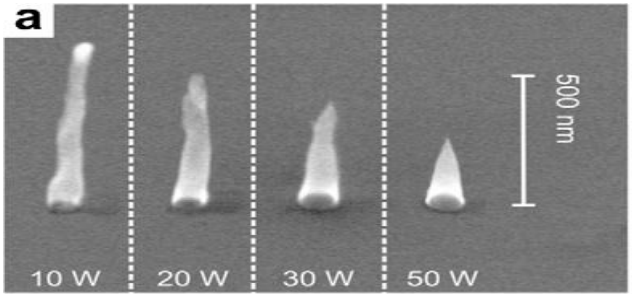

Fig.2.3.(i) Showing variation of power on CNT diameter.

2) Variation of Temperature

At higher temperatures of the substrate and catalyst the hydrocarbon gas dissociates faster, aided by the catalyst. A higher diffusion rate of carbon atoms through the catalytic particle can be expected, which results in considerably longer CNTs at the same growth time.

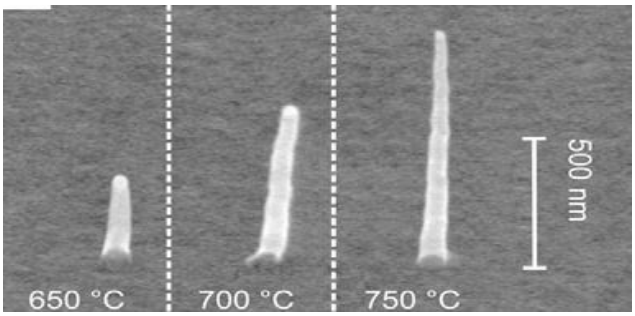

Fig.2.3.(ii) Showing variation of temperature on CNT length.

3) Variation of growth time

The CNT length is expected to depend linearly on growth time. CNTs grown at a process time of 5 min, 10 min, 15 min and 20 min confirm this linear dependence. Measurements on these CNTs yield a growth rate of 40 ± 5 nm/min. The low growth rate is a result of the low process temperature of 600ºC and low pressure of 4.3 mbar. In our PECVD process the CNT length is limited by the removal of the catalytic particle due to permanent sputtering during growth. Once the catalytic particle is removed, the CNT is etched back during the remaining process time. For the CNTs shown in figure the catalyst particle is still present in the tip of the CNTs.

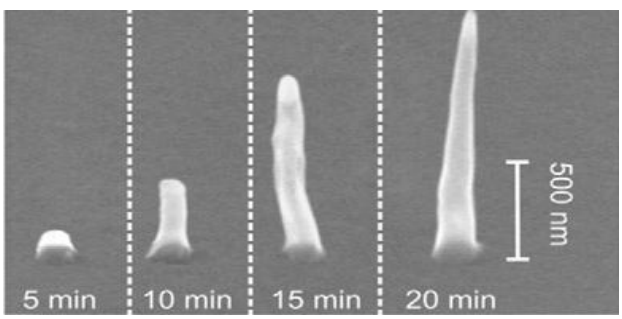

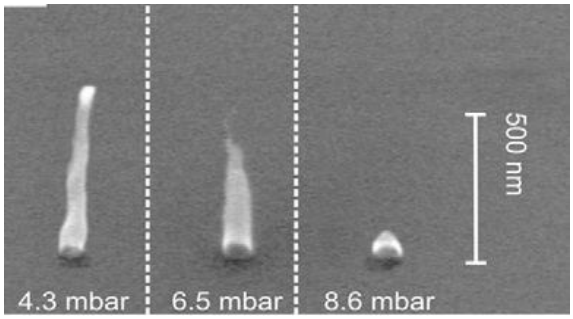

Fig. 2.3.(iii) Showing effect of variation of growth time and pressure on CNT growth.

4) Variation of Pressure

In thermal CVD growth of CNTs without the application of a plasma during growth the growth rate increases with higher pressure of the process gases acetylene and ammonia due to the increased density of hydrocarbon gas near the catalytic particle. We assume that the same mechanism also applies for plasma enhanced growth of CNTs. However, in the case of PECVD growth higher pressure also causes faster

back etching of the CNTs after reaching their maximum height due to the removal of the catalytic particle, leading to the results shown in figure.

2.4 Study of Effect of Plasma parameters on CNT growth (S.C. Sharma and Aarti Tewari *et.al Physics Of Plasmas 18, 063503 (2011)*

Carbon nanotubes (CNT) are being extensively studied because of their excellent properties. The growth mechanism of CNT in a plasma environment has been an important field of research in recent years. CNT of different shapes and sizes have been synthesized in a plasma environment. The effects of catalysts, growth temperature, the density of participating species, etc., have been extensively studied.

Suresh C. Sharma and Aarti Tewari [34] has recently researched upon the effect of plasma parameters (e.g., electron density and temperature, ion density and temperature, neutral atom density and temperature) on the growth (without a catalyst), structure, and field emission properties of a spherical carbon nanotube (CNT). A theoretical model of charge neutrality, including the kinetics of electrons, positively charged ions, and neutral atoms and the energy balance of the various species in plasma, has been developed. Numerical calculations of the radius of the spherical CNT tip for different CNT number densities and plasma parameters have been carried out for the typical glow discharge plasma parameters. It is found that upon an increase in the CNT number density and plasma parameters, the radius of the spherical CNT tip decreases, and consequently the field emission factor for the spherical CNT tip increases.

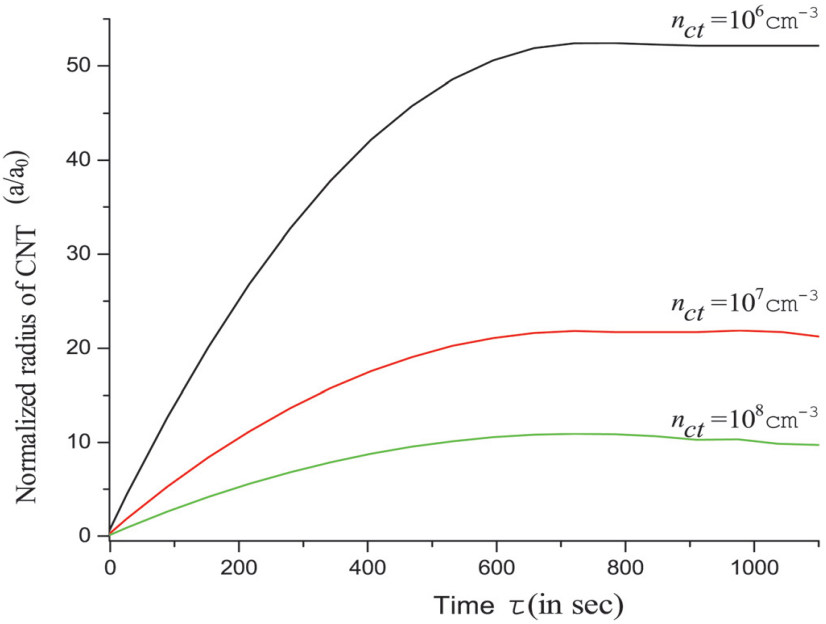

Fig.2.4.(i) Illustrates the variation of the normalized radius a=a0 of a spherical CNT tip with time for different CNT number densities (i.e., n_{ct}=106 cm^3, 107 cm^3, 108 cm^3) and for other parameters as mentioned above.

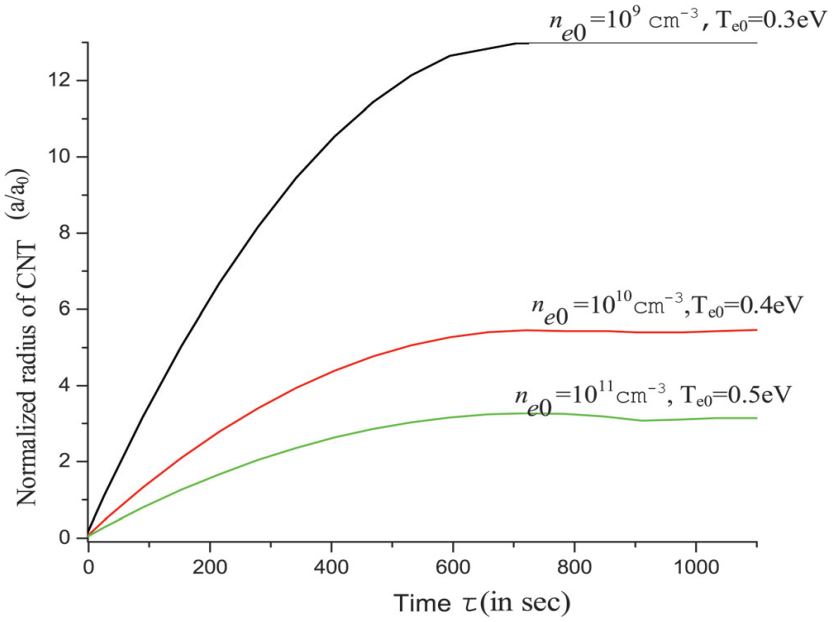

Figure 2.4.(ii) Shows the variation of the normalized radius a=a0 of a spherical CNT tip with time for different electron number densities and electron temperatures (e.g., n_{e0}=109 cm^3 and T_{e0}=0.3 eV, n_{e0}=1010 cm^3 and T_{e0}=0.4 eV, n_{e0} =1011 cm^3 and T_{e0}=0.5 eV).

2.5 Study Of Field Emission Of CNT By Various Authors

Field emission from Carbon Nanotubes (CNT) has been the topic of great interest to researchers across the world. There have been many advancements achieved in the recent past in controlling the properties of CNTs in order to get high emission results. Field emission from the CNTs allows us to use this extraordinary characteristic of CNT in developing the potential devices like Field emission displays, electron microscopes etc. Some work from various researchers is discussed below:

Choi *et al.*[35] have synthesized the vertically aligned CNT by thermal chemical vapour deposition(CVD) method and have studied the field emission properties by controlling the diameter of nanotubes. They found that the turn-on field is the lowest for the CNT grown on Iron (Fe) catalyst having 25nm thickness and it increases as the diameter increases. This suggests that the field emission from CNT have strong dependence on the nanotube diameters.

Kyung *et al.*[36] have studied the growth and field emission properties of MWCNTs by using atmospheric pressure PECVD and investigated the structural and electrical characteristics for its possible applications as field emitters in field emission display devices (FED). The results show the turn-on field

to be 2.92 V/μm, and the emission field at 1 mA/cm^2 to be 5.325 V/μm, which is appropriate for FED emitters.

Wang *et al.*[37] have grown Vertically aligned CNT films with diameters smaller than 5 nm and have investigated the electron field emission properties of the films by variable distance field emission and temperature-dependent field electron emission microscopy (T-FEEM). The films showed an emission site density of ~104/cm^2 and a threshold field of 2.8 V/μm. The results proved the strong dependence of size of CNT on its field emission properties.

Yu *et al.*[38] have reported the enhanced electron field emission of one-dimensional highly protruded graphene wrapped CNT Composites (GWCNT). The results depicts the best Field Emission (FE) performance for (Ruthenium)Ru-GWCNTs based emitters, with a turn on field of 0.61 V/μm, a current density of 2.5mA/cm^2 at a field of 1V/μm and a field enhancement factor of 6958.

Bonard *et al.*[39] have investigated the field emission properties of multiwalled CNT. Nanotubes have found to show high current densities at low operating voltages.

2.6 WHAT IS FIELD EMISSION?

Field emission (**FE**) is emission of electrons induced by an electrostatic field. The most common context is field emission from a solid surface into vacuum. However, field emission can take place from solid or liquid surfaces, into vacuum, air, a fluid, or any non-conducting or weakly conducting dielectric. The field-induced promotion of electrons from the valence to conduction band of semiconductors can also be regarded as a form of field emission.

Fowler–Nordheim (F–N) equation:

$$I = aV^2 \exp(-b\varphi^{3/2}/\beta V)$$

Where,
I, V, φ,β are the *emission current, applied voltage, Work function and field emission factor respectively.*

From **Wang *et al.*[40] J. Appl. Phys. 96, 6752 (2004),** it has been shown that field enhancement factor B depends upon length and radius of carbon nanotube as in the formula given :

$$\beta = \frac{h}{\rho} + 3.5,$$

Where,

h = height/length of CNT and ρ = radius of CNT

Field emission factor (β) depends upon :

1. Radius of CNT tip : sharp tips/ protrusions
2. Height/length of CNT : little effect on β

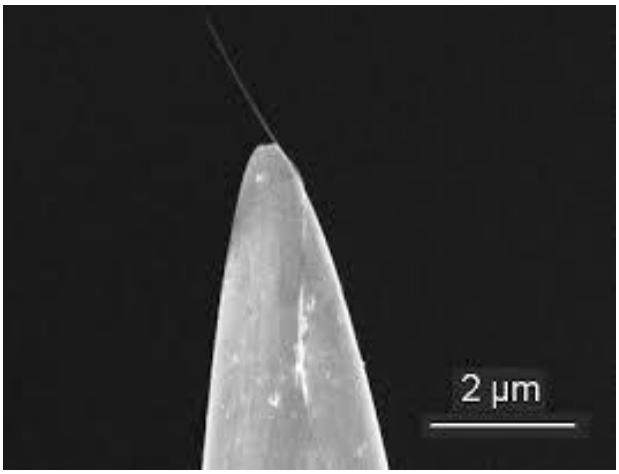

(a)

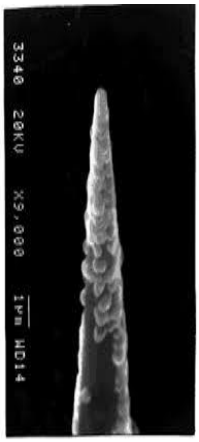

(b)

Fig. 2.6 (a) & (b) Showing TEM images of CNT

Fowler and Nordheim (FN) showed that, in the presence of an electric field, electrons tunnel out of the metal into the vacuum because of their quantum wave-like nature. However, comparison between calculated and observed currents reveals that emission at a given field is substantially higher than the FN predictions. Traditionally, the excess has been attributed to a field enhancement factor β_{FN} arsing from hypothetical asperities on the surface that supposedly enhance the electric field.

The use of CNTs as field electron emitters is considered as one of the most promising technological application due to the possibility of industrial production[41]-[45]. Indeed, CNTs are characterized by high emission electronic properties due to their good electron conductivity and a specific geometry, resulting in a drastic amplification of the electrical field strength in the vicinity of the nanotube tip [41]-[45].

In particular, the electron emitting properties of the CNT films result to be deeply affected by the overall organisation of the nanotubes (alignment degree, density, length, etc.) and on the quality and typology of the supporting material. In the case of a densely packed film, however, the number of CNTs involved in the electronic emission process is hard to estimate, with the additional complication that the emission capabilities of individual sites can vary widely, due to the dependence of the CNTs electronic properties on structural parameters as diameter, chirality, occurrence of structural defects, etc[46],[47].

It has also been proven that both the length (l) and the radius (r) of the tube play an important role in the Field Emission process, influencing both the field enhancement factor γ and the turn-on field Et

2.7 APPLICATION OF CNTs AS FIELD EMITTERS

The importance of investigating the behaviour of individual CNTs as field emitters is also related to their technological potentialities as nano-sized **electron sources** in developing high resolution **electron beam based instrumentation as displays[48]and electron microscopes[49]**.

2.7.(i) FIELD EMISSION DISPLAYS

Field Emission Display is consisted mainly with two pieces of glass substrate, and there are spacers between them. The space in between is vacuum. The front plate is called anode plate. On the anode plate, there are electrodes and phosphors that are illuminating by electrons impacting. The rear plate is cathode plate consisted of electrodes and field emission array (FEA) formed by large number of emitters that emitting electrons in accordance with field emission principles. The operating principle is that cathode emits electrons on the basis of the field emission principle and electrons are accelerated by electric field to impact fluorescent layer at anode plate and excite phosphors to illuminate. This illuminating principle is similar to conventional cathode ray tube (CRT), however, the electrons emitting way of field emission display is releasing by plane. By this way, it can make the conventional CRT flat and thin. This is why the field emission display is known as a thin CRT.

The difference between them is the electron releasing way of cathodes. CRT is hot electron generated by heating the cathode electron gun and deviation of electron is controlled by electromagnetic field to scan

fixed location on fluorescent screen, while field emission display cathode is formed with large number of emitter, which is virtually unnumbered micro electron gun. When electrons are emitted by field emission principle, they will be accelerated directly by electric field to hit on the corresponding pixels formed by phosphor. Therefore, Field Emission Display can maintain the image quality of CRT and improve the bulky size of it and making it thinner and lighter.

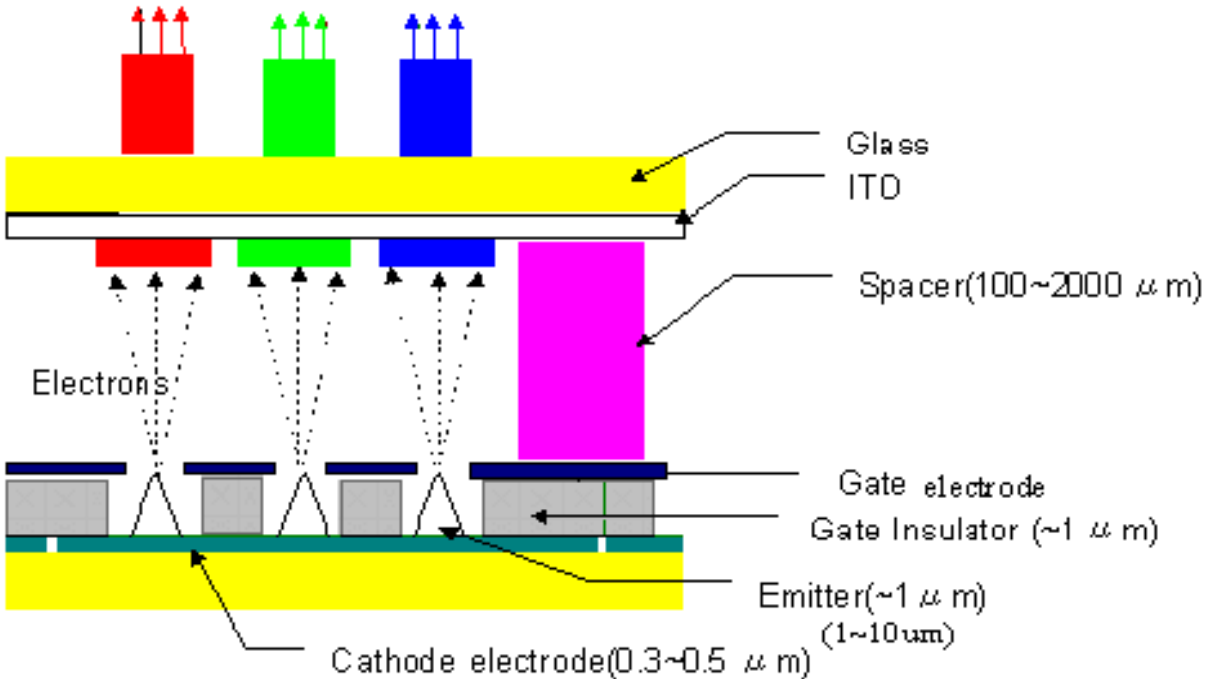

Fig. 2.7 Showing the CNT based Field emission display technology

SAMSUNG'S PROTOTYPE OF FIELD EMISSION DISPLAY USING ON CARBON NANOTUBE

Technology Review, November 2004,May 2005

2.8 DOPING ON CARBON NANOTUBES

The study of properties and applications of pristine C-NT has progressed enormously in the recent years and a great interest has been lately observed towards improving and controlling their properties through different functionalization methods. A modification of the crystalline nanotube properties by controllably placing defects or foreign atoms brings along tremendous technological implications [50-53]carbon [54], which justifies the number of experimental and theoretical investigations.

Nitrogen atoms incorporated in the C-NT structure represent for several reasons a practical and illustrative case. If a carbon single-walled nanotube (C-SWNT) is doped with a foreign N atom, its outstanding electronic properties differ drastically from an undoped C-SWNT. Even the cases of multiwalled (MW) and C-SWNTs doped with N are radically different. As compared to bulk doped carbons and also against other doped carbon layered structures, (i.e. bulk doped graphite), the electronic properties of C-NTs differ due to quantum confinement effects and the curvature of the cylinders.

Nitrogen contains one additional electron as compared to Carbon atom in carbon nanotube, thus novel electronic properties can be expected if Nitrogen atoms directly substitute Carbon atoms in the graphitic lattice and one could anticipate that they would generate an **N-type material** [55]. The electronic behaviour depends on the new geometry generated which involves a different wall structure and different size of the lattice. Thereby brining in changes in the field enhancement factor of the carbon nanotubes. One cannot discard that this new arrangement makes a p-type doping also feasible**. P-type** doping is done by using Boron as heteroatom in the crystal lattice of carbon nanotubes. The addition of Boron also suggests some geometrical changes like in the radius, the length etc. However , change in length with doping has not given any substantial results so far.

CHAPTER 3: RESEARCH WORK

3.1 TOPIC :

EFFECT OF DOPING ON GROWTH AND FIELD EMISSION PROPERTIES OF SPHERICAL CARBON NANOTUBE (CNT) TIP PLACED OVER CYLINDRICAL SURFACE

Carbon Nanotubes (CNTs) have been the subject of widespread research due to its exceptionally advanced properties and its vast number of potential applications like in microelectronics as CNT Field effect transistors (CNTFETs) for energy storage as Lithium ion batteries etc. In the recent years a great interest has developed towards improving and controlling their properties through different functionalization methods. Some results have shown the effect of controlled size on the field emission properties of CNTs[35,36,37]. There can be ways which can instill changes in the properties especially the field emission of CNTs by controllably placing defects or the hetero-atoms in the crystal lattice of carbon.[56,57,58]

Some articles published recently have shown the effect of N and B on structural changes of CNT and have estimated that N doping decreases the size of CNT and B doping increases the size of CNT[56,58]. Moreover, N doped CNTs have found to show enhanced field emission properties because of the presence of an external additional electron in the crystal lattice of carbon and a strong dependence of field emission from CNT on its radius has been established[57,58]. The incorporation of hetero-atoms like Nitrogen (N) and Boron (B) adds and removes an electron from the carbon lattice, respectively, thereby bringing novel changes in the electronic and optical properties of CNTs. Some work has also been done to study the advantages of growing CNT in plasma environment and various parameters like temperature, plasma power, and number density of electrons, ions etc. and other parameters affecting its properties[33,34].

Choi *et al.*[35] have synthesized the vertically aligned CNT by thermal chemical vapour deposition(CVD) method and have studied the field emission properties by controlling the diameter of nanotubes. They found that the turn-on field is the lowest for the CNT grown on Iron (Fe) catalyst having 25nm thickness and it increases as the diameter increases. This suggests that the field emission from CNT have strong dependence on the nanotube diameters.

Kyung *et al.*[36] have studied the growth and field emission properties of MWCNTs by using atmospheric pressure PECVD and investigated the structural and electrical characteristics for its possible applications as field emitters in field emission display devices (FED). The results show the turn-on field to be 2.92 V/μm, and the emission field at 1 mA/cm^2 to be 5.325 V/μm, which is appropriate for FED emitters.

Wang *et al.*[37] have grown Vertically aligned CNT films with diameters smaller than 5 nm and have investigated the electron field emission properties of the films by variable distance field emission and temperature-dependent field electron emission microscopy (T-FEEM). The films showed an emission site density of ~104/cm^2 and a threshold field of 2.8 V/μm. The results proved the strong dependence of size of CNT on its field emission properties.

Koos *et al.*[56] have investigated the effect of the reaction parameters on the structure of multi-walled carbon nanotubes (MWCNTs) containing different concentrations of nitrogen and boron. It has been shown that doping CNT with heteroatoms, such as B and N, can be used to control nanotube diameters.

Padya *et al.*[57] fabricated well-aligned nitrogen-doped CNT (N-CNTs) film was on silicon substrate by thermal chemical vapor deposition process with varying the growth temperature. The effect of growth temperature on morphology, microstructure and crystallanity for the growth of N-CNTs was studied. Field emission study of nitrogen-doped CNT grown at optimum parameters showed that they are good emitters with a turn-on and threshold field of 0.3 and 1.6 V/μm, respectively. They found that the compartment distance decreases with increase in nitrogen doping level in hexagonal graphite network.

Srivastava *et al.*[58] have studied the enhanced field emission characteristics of nitrogen-doped carbon nanotube films grown by microwave plasma enhanced chemical vapor deposition(MPECVD) process. In this case CNTs obtained had bamboo structure with very sharp tips. These films showed very good field emission characteristics with threshold field in the range of 2.65–3.55 V/μm. They have also found that CNT doped with N helps in re-nucleation of new compartments with wall thickness at the joint section being more and decreases towards the base in the growth model of the bamboo shaped structure.

Sharma and Tewari [34] have investigated the effect of plasma parameters on the growth and field emission properties of CNT. The results have shown that the radius of spherical CNT tip decreases with plasma parameters i.e. number density of CNT, electron and ion number density, and temperatures.

Loffler *et al.*[33] have experimentally shown the various factors affecting the growth of CNT. They have presented the systematic variation of PECVD factors like power, temperature, pressure and

growth time which resulted in the increase or decrease of the length of CNT.

We study the effect of doping on the growth (without catalyst) and field emission properties of a spherical CNT tip placed over the cylindrical surface. In Chapter 2, we develop a theoretical model for the spherical CNT tip placed over cylindrical surfaces based on the charge neutrality of the spherical CNT tip placed over the cylindrical surface, including the kinetics of various species in plasma, e.g., electrons, neutral atoms, positively charged ions including doping atoms as N and B , and number density of the spherical CNT tip placed over cylindrical surfaces, and the energy balance of the various plasma species, and the spherical CNT tip placed over the cylindrical surface. Results and discussions are given in Chapter 3. Finally, the conclusion part is given in Section 3.4.

3.2 RESEARCH METHODOLOGY

3.2.(i) MODEL

Following Sodha *et al*.[59,60] and Tewari *et al*.[61],we consider plasma containing electrons, positively charged ions of type A , B and C, neutral atoms of type A, B and C, and CNT with spherical tip placed over the cylindrical surface is grown (without catalyst) in the presence of plasma. The positively charged ions are assumed to be singly ionized. A refers to Carbon ions, B refers to Neon and C refers to the doped atoms, i.e., Nitrogen (N) and Boron (B) in our case.

Plasma containing electrons, neutral atoms and positively charged ions of TYPE A, B and C

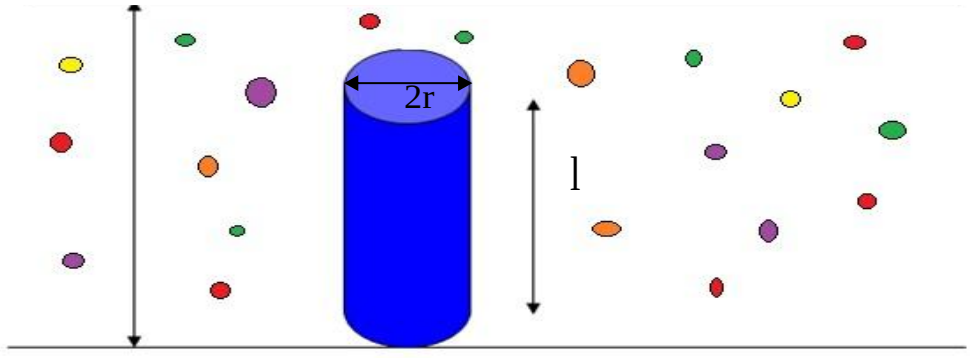

Fig.3.2 CNT tip Placed Over Cylindrical Surface in the presence of Plasma

The initial radius of CNT r_0 (same for spherical tip and cylindrical surface) can be estimated by equating the accretion of electrons and positively charged ions on the CNT, i.e.,

$$4\pi {r_0}^2 n_e \left(\frac{T_e}{m_e}\right)^{\frac{1}{2}} \exp\left(-\frac{e^2}{r_0 k_B T_e}\right) + 2\pi r_0 l_0 n_e \left(\frac{T_e}{m_e}\right)^{\frac{1}{2}} \exp\left(\frac{eV_s}{k_B T_e}\right) = \pi r_0^2 \left(1+\frac{e^2}{r_0 k_B T_i}\right)$$
$$\left[n_{iA}\left(\frac{T_i}{m_{iA}}\right)^{\frac{1}{2}} + n_{iB}\left(\frac{T_i}{m_{iB}}\right)^{\frac{1}{2}} + n_{iC}\left(\frac{T_i}{m_{iC}}\right)^{\frac{1}{2}}\right] + \left[n_{iA}\left(\frac{T_i}{m_{iA}}\right)^{\frac{1}{2}} + n_{iB}\left(\frac{T_i}{m_{iB}}\right)^{\frac{1}{2}} + n_{iC}\left(\frac{T_i}{m_{iC}}\right)^{\frac{1}{2}}\right]$$
$$\left[\frac{2}{\sqrt{\pi}}\left(\frac{eV_s}{k_B T_i}\right)^{\frac{1}{2}} + \exp\left(\frac{eV_s}{k_B T_i}\right) erfc\left(\frac{eV_s}{k_B T_i}\right)^{\frac{1}{2}}\right].$$

(1)

In Eq. (1)

l_0 = length of CNT,

V_s = the surface potential on the cylindrical CNT

n_e = number density of electron,

T_e = electron temperature,

k_B = Boltzmann's constant,

T_i = ion temperature,

n_{iA} = number density of ion A, where A refers to Carbon

m_{iA} = mass of ion A,

n_{iB} = number density of ion B, where B refers to Neon

m_{iB} = mass of ion B,

n_{iC} = number density of ion C, where C refers to either Nitrogen or Boron

m_{iC} = mass of ion C, where C refers to either Nitrogen or Boron

e = electronic charge.

A. Charge neutrality equation

$$Zn_{ct} + n_{iA} + n_{iB} + n_{iC} = n_e, \quad (2)$$

where

Z= charge on CNT,

n_{ct} = number density of CNT.

B. Charging of the CNT

This equation describes the charge developed on the CNT due to accretion of electrons and positively charged ions on the surface of CNT.

$$\frac{dZ}{d\tau} = n_{iActs} + n_{iActcys} + n_{iBcts} + n_{iBctcys} + n_{iCcts} + n_{iCctcys} - \gamma_e\left(n_{ects} + n_{ectcys}\right), \quad (3)$$

where

$n_{ects} = \pi r^2 \left(\frac{8k_B T_e}{\pi m_e}\right)^{\frac{1}{2}} n_e \exp\left[Z\alpha_e\right]$ is the electron collection current at the surface of spherical CNT tip and $\alpha_e\left(=\frac{e^2}{rk_B T_e}\right)$,

$n_{ijcts} = \pi r^2 \left(\frac{8k_B T_i}{\pi m_j}\right)^{\frac{1}{2}} n_{ij}\left[1 - Z\alpha_i\right]$ is the ion collection current to spherical CNT .

For surface of cylindrical CNT

$n_{ectcys} = n_e rl\left(\frac{2\pi k_B T_e}{m_e}\right)^{\frac{1}{2}} \exp\left[\frac{eV_S}{k_B T_e}\right]$ is the electron collection current at the surface of cylindrical CNT.

$$n_{ijctcys} = n_{ij} rl\left(\frac{2\pi k_B T_i}{m_{ij}}\right)^{\frac{1}{2}} \left\{\frac{2}{\sqrt{\pi}}\left(\frac{eV_S}{k_B T_i}\right)^{\frac{1}{2}} + \exp\left[\frac{eV_S}{k_B T_i}\right] erfc\left[\left(\frac{eV_S}{k_B T_i}\right)^{\frac{1}{2}}\right]\right\}$$

is the ion collection current at the surface of cylindrical CNT.

and $\alpha_i\left(=\frac{e^2}{rk_BT_i}\right)$, r is the radius of spherical CNT tip placed over cylindrical CNT surface, γ_e is the sticking coefficient of constituent electron at the surface of spherical CNT tip , j refers to either A or C positively charged ion , A and C are same as described in Eq.(1).

C. Growth rate equation of electron density

The equation describes the growth rate of electron density in the plasma

$$\frac{dn_e}{d\tau}=\left(\beta_A n_A+\beta_B n_B+\beta_C n_C\right)-\left(\alpha_A n_e n_{iA}+\alpha_B n_e n_{iB}+\alpha_A n_e n_{iC}\right)-\gamma_e n_{ct}\left(n_{ects}+n_{ectcys}\right), \quad (4)$$

where

A in n_A refers to Carbon atoms.

β_j is the coefficient of ionization of the constituent neutral atoms due to external agency, $\alpha_j(T_e)=\alpha_{j0}\left(\frac{300}{T_e}\right)^{\kappa} cm^3/\sec$ is the coefficient of recombination of electrons and positively charged ions. The first term in Eq.(4) is the rate of gain in electron density per unit time on account of ionization of neutral atoms and second term is the decaying rate of the electron density due to electron – ion recombination and the third term is the electron collection current at the surface of CNT.

D. Growth rate equation of positively charged ion density

The equation describes the growth rate equation of positively charged ions in plasma

$$\frac{dn_{iA}}{d\tau}=\beta_A n_A-\alpha_A n_e n_{iA}-n_{ct}\left(n_{iActs}+n_{iActcys}\right), \quad (5)$$

$$\frac{dn_{iB}}{d\tau}=\beta_B n_B-\alpha_B n_e n_{iB}-n_{ct}\left(n_{iBcts}+n_{iBctcys}\right), \quad (6)$$

$$\frac{dn_{iC}}{d\tau}=\beta_C n_C-\alpha_C n_e n_{iC}-n_{ct}\left(n_{iCcts}+n_{iCctcys}\right). \quad (7)$$

The first term in Eqs.(5), (6) & (7) is the gain in ion density per unit time on account of ionization of

neutral atoms, second term is the electron-ion recombination and third term is the ion collection current to the surface of CNT.

E. Growth rate equation of neutral atoms

The equation describes the growth rate equation of neutral atoms in plasma

$$\frac{dn_A}{d\tau} = \alpha_A n_e n_{iA} - \beta_A n_A + n_{ct}\left(1-\gamma_{iA}\right)\left(n_{iActs} + n_{iActys}\right) - n_{ct}\gamma_A\left(n_{Acts} + n_{Actcys}\right), \tag{8}$$

$$\frac{dn_B}{d\tau} = \alpha_B n_e n_{iB} - \beta_B n_B + n_{ct}\left(n_{iBcts} + n_{iBctcys}\right), \tag{9}$$

$$\frac{dn_C}{d\tau} = \alpha_C n_e n_{iC} - \beta_C n_C + n_{ct}\left(1-\gamma_{iC}\right)\left(n_{iCcts} + n_{iCctys}\right) - n_{ct}\gamma_C\left(n_{Ccts} + n_{Cctcys}\right), \tag{10}$$

where

$n_{jcts} = \pi r^2 \left(\frac{8k_B T_n}{\pi m_j}\right)^{\frac{1}{2}} n_j$ is the neutral collection current at the surface of spherical CNT tip and for cylindrical CNT $n_{jctcys} = \pi a l \left(\frac{2k_B T_n}{m_j}\right)^{\frac{1}{2}} n_j$ is the neutral collection current . The first term in Eqs. (8), (9) & (10) is the gain in neutral atom density per unit time due to electron–ion recombination, second term is the decrease in neutral density due to ionization, third term is the gain in neutral density due to neutralization of the atoms collected at the surface of CNT and the last term in Eq. (8) & (10) is the accretion of neutral atoms of species A and C on the surface of CNT.

F. Growth rate equation of the mass of CNT

$$\frac{dm_{ct}}{d\tau} = \begin{bmatrix} m_A\gamma_A\left(n_{Acts} + n_{Actcys}\right) + m_{iA}\gamma_{iA}\left(n_{iActs} + n_{iActcys}\right) + \\ m_C\gamma_C\left(n_{Ccts} + n_{Cctcys}\right) + m_{iC}\gamma_{iC}\left(n_{iCcts} + n_{iCctcys}\right) \end{bmatrix}, \tag{11}$$

$m_{ct} = \frac{4}{3}\pi r^3 \rho_{ct} + \pi r^2 l \rho_{ct}$ is the mass of the CNT and ρ_{ct} is the density of CNT. The terms are the gain in mass density due to collection of atomic and ionic species of A and C

H. Field enhancement factor β

Using the expression for field enhancement factor obtained by Wang *et al.*[40]

$$\beta = \frac{h}{\rho} + 3.5, \tag{13}$$

where

h = height of CNT and ρ = radius of CNT

3.3 RESULTS AND DISCUSSIONS

The thesis presents a theoretical model for understanding the growth of Carbon Nanotubes (CNTs) in complex plasma on account of effect of hetro-atoms such as N and B on CNT surface. The charging of CNT, kinetics of electrons, neutral atoms, mass and energy balance of CNT with spherical tip placed over the cylindrical surface in the presence of N and B has been incorporated in the model. There are many ways in which the growth of CNTs in a complex plasma environment can occur namely cluster formation, nucleation, coagulation, and growth of embryonic nanotubes by condensation. Although other processes are equally important but in the present investigation we study the growth of embryonic nanotubes by condensation in a complex plasma because we are interested to study how the growth process of CNT is affected by hetero atoms such as N and B which can be treated as doping elements on CNT surface. We assume that electrons in the plasma ionize the neutral atoms producing positively charged ions and electrons. Various processes like ionization (in which an atom or a molecule acquires a negative or positive charge by gaining or losing electrons), recombination (in which positive ions of a plasma capture a free electron and combine with electrons or negative ions to form new neutral atoms) and sticking of plasma species on CNT contributing to its growth have been considered.

Numerical calculations have been carried out to study the growth of CNTs on account of hetro-atoms such as N and B treated as doping elements on CNT surface. Electron temperature (T_e), neutral atom temperature (T_n), ion temperature (T_i), CNT number density (n_{ct}) are fixed and number density of

electron(n_e), number density of ions (n_i), number density of neutral atom (n_n) for Carbon, Nitrogen and Boron have been varied to obtain the effect of addition of N and B on the normalized radius of spherical CNT tip placed over the cylindrical surface .This is because the number density of electrons, ions and neutral atoms changes with doping.

1. **By taking boundary conditions and other relevant plasma parameters for undoped spherical CNT at,**

$\tau = 0$, number density of CNT , i.e., n_{ct} =10^6 cm^{-3} , number density of ion A and B, i.e., $n_{iA0} = n_{iB0} = 10^8$ cm^{-3}, number density of neutral atoms A and B, i.e., $n_{A0} = n_{B0} = 5\times10^9$ cm^{-3},number density of electron ,i.e., $n_{e0} = 10^8$ cm^{-3}, electron temperature in absence of CNT, i.e., $T_{e0} = 0.5$ eV, ion temperature, i.e., $T_{i0} = 2500$ K, neutral atom temperature, i.e., T_{n0}=CNT temperatureT_{ct} =2000K , mass of ion A, i.e., $m_{iA} \approx m_A$ =12 amu (Carbon), mass of ion B, i.e., $m_{iB} \approx m_B$ = 20 amu (Neon). Other parameters are coefficient of recombination of electrons and ions of type A and B, i.e., $\alpha_{A0} \approx \alpha_{B0}$ =$10^{-7}$$cm^3$/sec, emissivity of the material of CNT, i.e., ε =0.6 , sticking coefficient of ion A and neutral atom A at the surface of CNT, i.e., $\gamma_{iA} = \gamma_A$ =1, work function of CNT, i.e., $\phi = 4.8$ eV (Carbon)[62], specific heat of CNT $C_p = 7\times10^6$ ergs/gK, ionization energy of neutral atom A, i.e., I_{pA} =11.26 eV, ionization energy of neutral atom B, i.e., I_{pB} =10eV , mean energy of electron produced by ionization of neutral atom A/B, i.e., ε_A =6.2 eV and ε_B =10.7 eV, mean energy of positively charged ions A/B produced by ionization of neutral atom, i.e., ε_{iA} =7.3 eV and ε_{iB} = 12.2 eV , κ = -1.2,initial radius of CNT r_0= 0.7nm and density of CNT, i.e., ρ_{ct} = 4.2g/cm^3.

2. **Calculations for doped- Nitrogen (N) CNTs using boundary conditions at,**

$\tau = 0, n_{ct}$ =10^6 cm^{-3} , $n_{iA0} = n_{iB0} = n_{iC0} = 10^9$ cm^{-3}, $n_{e0} = 10^9$ cm^{-3},

$n_{A0} = n_{B0} = n_{C0} = 5\times10^8$ cm^{-3}, $T_{e0} = 1.5$eV, $T_{i0} = 2600$ K , $T_{n0} = T_{ct} = 2100$ K.

$m_{iA} \approx m_A$ =12 amu (Carbon) , $m_{iB} \approx m_B$ = 20 amu (Neon), $m_{iC} \approx m_C = 14$amu (Nitrogen).

Other parameters are

$\alpha_{A0} \approx \alpha_{B0}$ =1.56×10^{-7}cm^3/sec, ε =0.6, $\gamma_{iA} = \gamma_A$ =1, ϕ = 4.62 eV (Nitrogen) as Zhang *et al.*[62] suggests that there is a decrease in work function by 0.18eV on addition by N as compared to pristine CNT , $C_p = 7\times10^6$ ergs/gK, I_{pA} = 12.32 eV, I_{pB} =11.21eV,I_{pC} =11.24 eV, ε_A =6.43 eV, ε_B =10.98 eV, ε_C =9.43 eV, ε_{iA} =7.3 eV, ε_{iB} = 12.76 eV , ε_{iC} =7.7 eV, κ = -1.2, r_0= 0.5nm and ρ_{ct} = 4.2g/cm^3.

3. Calculations for doped -Boron (B) CNTs using boundary conditions at,

$\tau = 0, n_{ct}$ =10^6 cm^{-3}, $n_{iA0} = n_{iB0} = n_{iC0} = 10^7$ cm^{-3}, $n_{A0} = n_{B0} = n_{C0} = 5\times10^{10}$ cm^{-3}, $n_{e0} = 10^7$ cm^{-3}, $T_{e0} = 1.3$eV, $T_{i0} = 2400$ K , $T_{n0} = T_{ct} = 1950$ K.

$m_{iA} \approx m_A$ =12 amu (Carbon) , $m_{iB} \approx m_B$ = 20 amu (Neon), $m_{iC} \approx m_C = 10.8$ amu (Boron).

Other parameters are

$\alpha_{A0} \approx \alpha_{B0}$ =1.08×10^{-7}cm^3/sec, ε =0.6 , $\gamma_{iA} = \gamma_A$ =1, ϕ = 4.9 eV (Boron) as Zhang *et al.*[62] suggests that there is a increase in work function by 0.1eV on addition by B as compared to pristine CNT, $C_p = 7\times10^6$ ergs/gK, I_{pA} = 10.34 eV, I_{pB} =9.56eV , I_{pC} =10.21 eV, ε_A =6.1 eV, ε_B =10.3 eV, ε_C =8.2 eV, ε_{iA} =6.8 eV, ε_{iB} = 11.23 eV , ε_{iC} =6.5 eV , κ = -1.2, r_0= 1.26nm and ρ_{ct} = 4.2g/cm^3.

Fig.3.3 illustrates the variation of normalized radius r/r_0 of CNT with spherical tip placed over the cylindrical surface with time for undoped CNT for the parameters mentioned in point no. **1**. From Fig.3.3, it can be seen that the value of normalized radius increases with time and after some time it attains a saturation value. This happens because as the time increases, the accretion of neutral atoms of carbon leads to the growth of CNT tip and therefore the normalized radius increases. The main parameters that determine the growth pattern going into the plateau region are the values of sticking coefficients of neutral atoms and ions of type A and the charge developed on the CNT. Because the value of sticking coefficients of neutral atoms and ions increases, the steady state is achieved faster. Also, as more and more neutral atoms and positively charged ions stick on the CNT surface, the negative charge on the CNT decreases, which further stops the accretion of ions and neutral atoms on the surface of the CNT and the CNT radius saturates[34].

Fig.3.4 display the time evolution of normalized radius r/r_0 of CNT with spherical tip placed over the cylindrical surface with N acting as dopant for parameters mentioned in point no. **2**. From Fig.3.4, it can be seen that the normalized radius of CNT display the same growth pattern as in Fig.1 but the

nanotube with N as doping element on CNTs surface has much lesser radius compared to undoped CNT. There can be many explanations to the reduced growth of CNT with N on its surface acting as dopant. One such explanation for the decreased value of the CNT tip radius with N at its surface is that with the presence of N atom on CNT surface produces an extra electron in the CNT lattice after covalently bonding with C of CNT. This extra electron ionizes the neutral atom present on the crystal lattice thereby decreasing the density of neutral atoms. Since it is the accretion of neutral atom on CNT which determines its growth, the radius of spherical CNT tip placed over the cylindrical surface with N acting as dopant decreases. The reduced growth of CNT with N can also be attributed to the etching of CNT by N but in present times etching of CNT by Hydrogen has attracted many researchers whereas little work has been done to highlight etching of CNT due to N. Some work in this regard has been done by Wen *et al*.[63]

Fig.3.5 illustrates the variation of the normalized radius r/r_0 of spherical CNT tip placed over the cylindrical surface with time with B acting as dopant for parameters mentioned in **3**. From Fig.3.5 it can be seen that the nanotube with B as doping element on CNTs surface has larger radius compared to undoped CNT and doped N. The CNT tip radius increases in Fig.3.5 because B engulfs an electron from the CNT lattice due to covalent bonding of B and C on CNT lattice, thereby reducing the electron number density and hence the ionization of neutral atoms also reduces. Since it is the accretion of neutral atom on CNT which determines its growth, the radius of spherical CNT tip placed over the cylindrical surface with B as doping element increases due to the reduced ionization of neutral atoms.

The results obtained in Figs.3.4 and 3.5 are in accordance with the study of Koos *et al.*[56] .They have obtained similar trends of CNT diameters due to N and B doping. They have shown that N slows down the nanotube formation significantly, which leads to shorter tubes. B doped nanotubes formed a several mm thick elastic soot layer, which may be an indication that B doping considerably increased the length of carbon Nanotubes.

Fig.3.6 shows the variation of normalized ion density of Carbon undoped CNT, Nitrogen-doped CNT, and Boron-doped CNT with time. A comparison has been made for the decay of ion density for undoped CNT, Nitrogen-doped CNT, and Boron-doped CNT. It has been shown that N ion decays faster followed by C and B ions. Since addition of N increases electron number density and electron number density decreases for B as explained above for Figs.3.4 &3.5, the ions of N decays faster compared to those of B and C ions. So, with an increase in electron number density, ions contributing to growth of CNT decays faster in case of N-doped CNT leading to lesser CNT radius and vice-versa for B-doped CNT .Our theoretical results are in accordance with the experimental observations of Lee *et a1*.[64] and

Srivastava *et al.*[65]

From the results obtained, the variation of the field emission factor with doping elements Nitrogen (N) and Boron (B) can be estimated. Since the field emission factor $\beta \propto \frac{1}{r}$ **(**where *l* is the length of CNT and *r* is the radius of the CNT). Using Eq.13 we have roughly estimated the field enhancement factor for all the three CNTs, i.e., undoped CNT, N-doped CNT and B-doped CNT. (cf. Fig. 3.7) .We calculate the radius of CNT for all three types of CNTs as 29.4nm for Undoped CNT, 5nm for N-doped CNT, 65.52nm for B-doped CNT , height of CNT is taken to be 15 μm, the field enhancement factor are obtained as 510.20 for Undoped CNT, 3000 for N-doped CNT, 228.93 for B-doped CNT. It can be seen from Fig.3.7 that N-doped CNT has highest field enhancement factor followed by Undoped and B-doped. Nitrogen is seen to improve field emission characteristics of CNT and B impedes the field emission from CNT.

We assume length of CNT at 5 μm, 10 μm, 15 μm, 20 μm and 25 μm and fix the radius of CNT to be 0.5nm,to understand the variation in field emission factor β with length for all the three types of CNTs, i.e., undoped CNT, N-doped CNT and B-doped CNT and obtained β as 220.34, 225, 228.93, 230, 232 (for Boron doped CNT), 448.10, 503, 510.20, 512.3,515(for Undoped CNT) and 2890,2998,3000,3012,3015 (for Nitrogen doped CNT) at length of CNT5 μm, 10 μm, 15 μm, 20 μm and 25 μm, respectively. Fig.3.8 illustrates the variation of field emission factor β with respect to different lengths of CNT for all three cases i.e. undoped CNT, Boron doped CNT and Nitrogen doped CNT. From Fig.3.8, we can conclude that length has little influence on the field emission factor β of CNT. The results obtained have also been experimentally observed by Xu *et al.*[66] [cf. Fig. 4(a) on page 133107-3].

Hence, assuming fixed length of CNT, $\beta \propto \frac{1}{r}$, so treating CNT with different elements (like Nitrogen, Boron) leads to larger β . The variation of β with CNTs radius has also been experimentally verified by Xu *et. Al.*[66] [cf. Fig. 4(b) on page 133107-3].

This result is similar to the experimental observations of Padya *et al.*[57], Srivastava *et al.*[58], Chan *et al.*[67] and Zhang *et al.*[68] .Therefore doping of CNT tip with Nitrogen atom can lead to enhanced field emission properties, a phenomenon which is not seen in the pristine CNT.

Undoped CNT

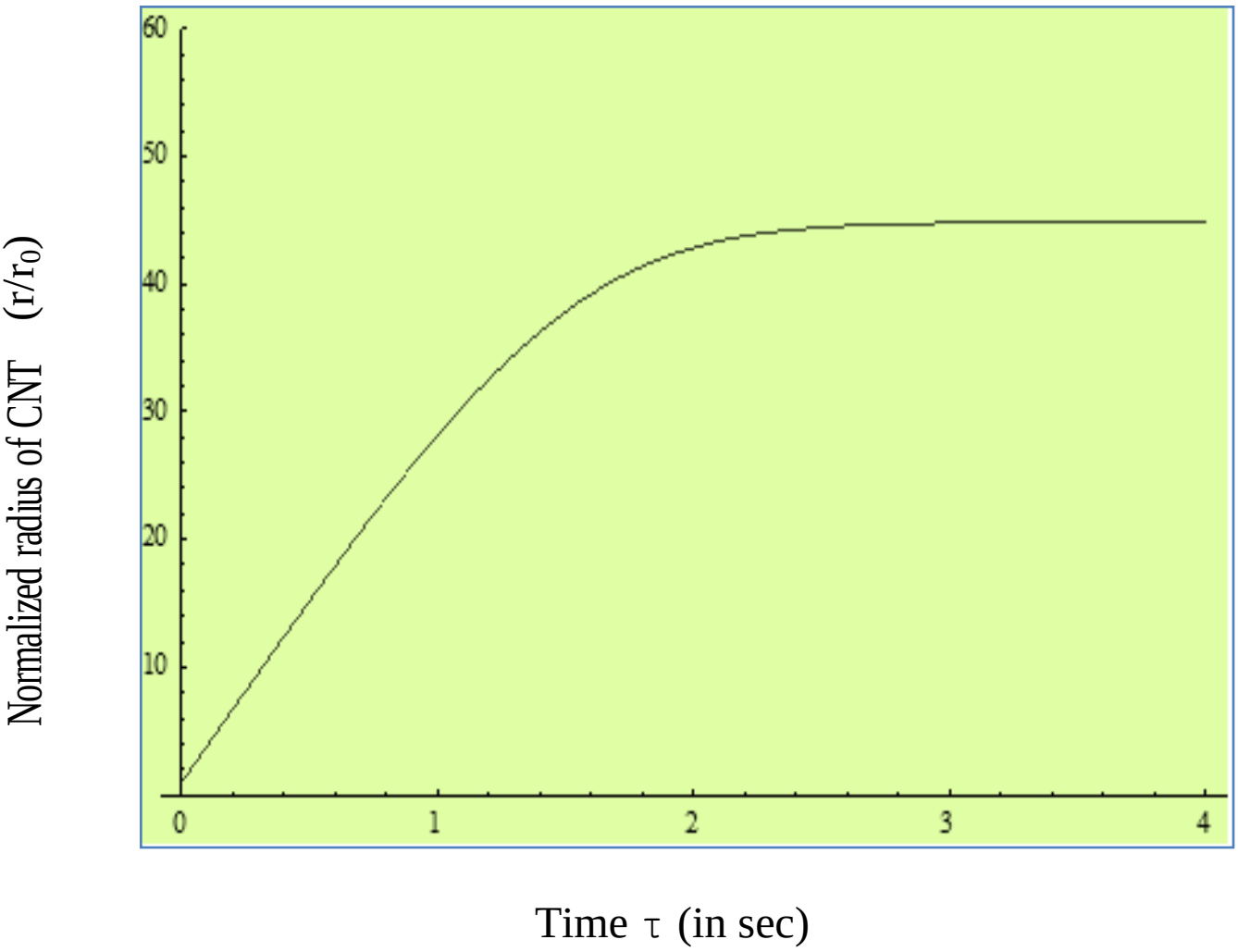

Fig.3.3: Shows the variation of the normalized radius r/r_0 of spherical CNT tip placed over cylindrical surface for undoped CNT using parameters (n_{ct}=10^6 cm^{-3} , n_{iA0} = n_{e0} = n_{iB0} =10^8cm^{-3}, $n_{A0} = n_{B0} = 10^9$ cm^{-3}, $T_{e0} = 0.5$ eV, $T_{i0} = 2500$ K, $T_{n0} = T_{ct} = 2000$ K).

Nitrogen-doped CNT

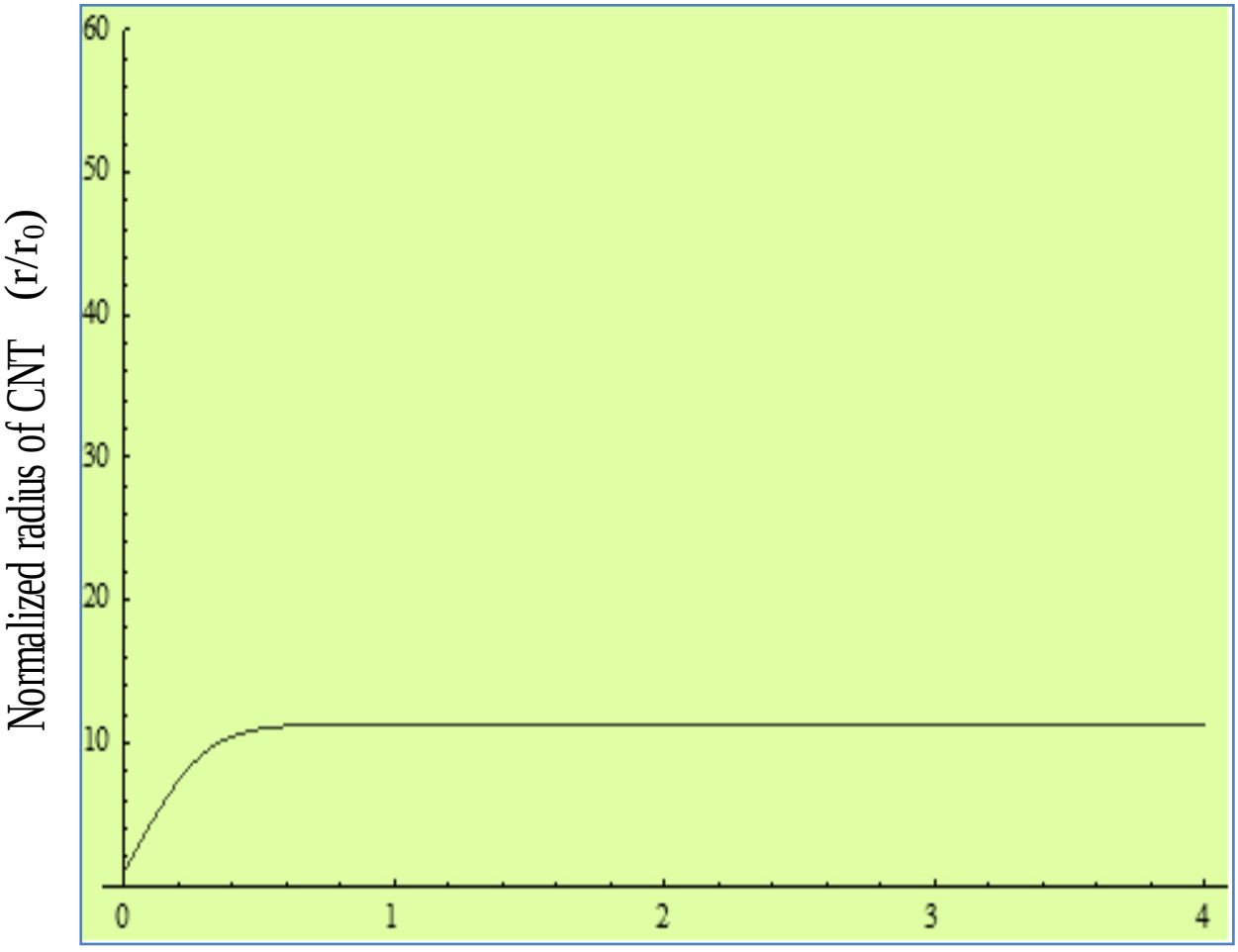

Fig.3.4: Shows the variation of the normalized radius r/r_0 of spherical CNT tip placed over cylindrical surface for doped Nitrogen using the parameters as ($n_{ct}=10^6 \text{cm}^{-3}, n_{iA0}=n_{iB0}=n_{iC0}=10^9 \text{ cm}^{-3}, n_{A0}=n_{B0}=n_{C0}=10^8 \text{ cm}^{-3}, n_{e0}=10^9 \text{ cm}^{-3}, T_{e0}=1.5\text{eV}, T_{i0}=2600$ K , $T_{n0}=T_{ct}=2100$ K).

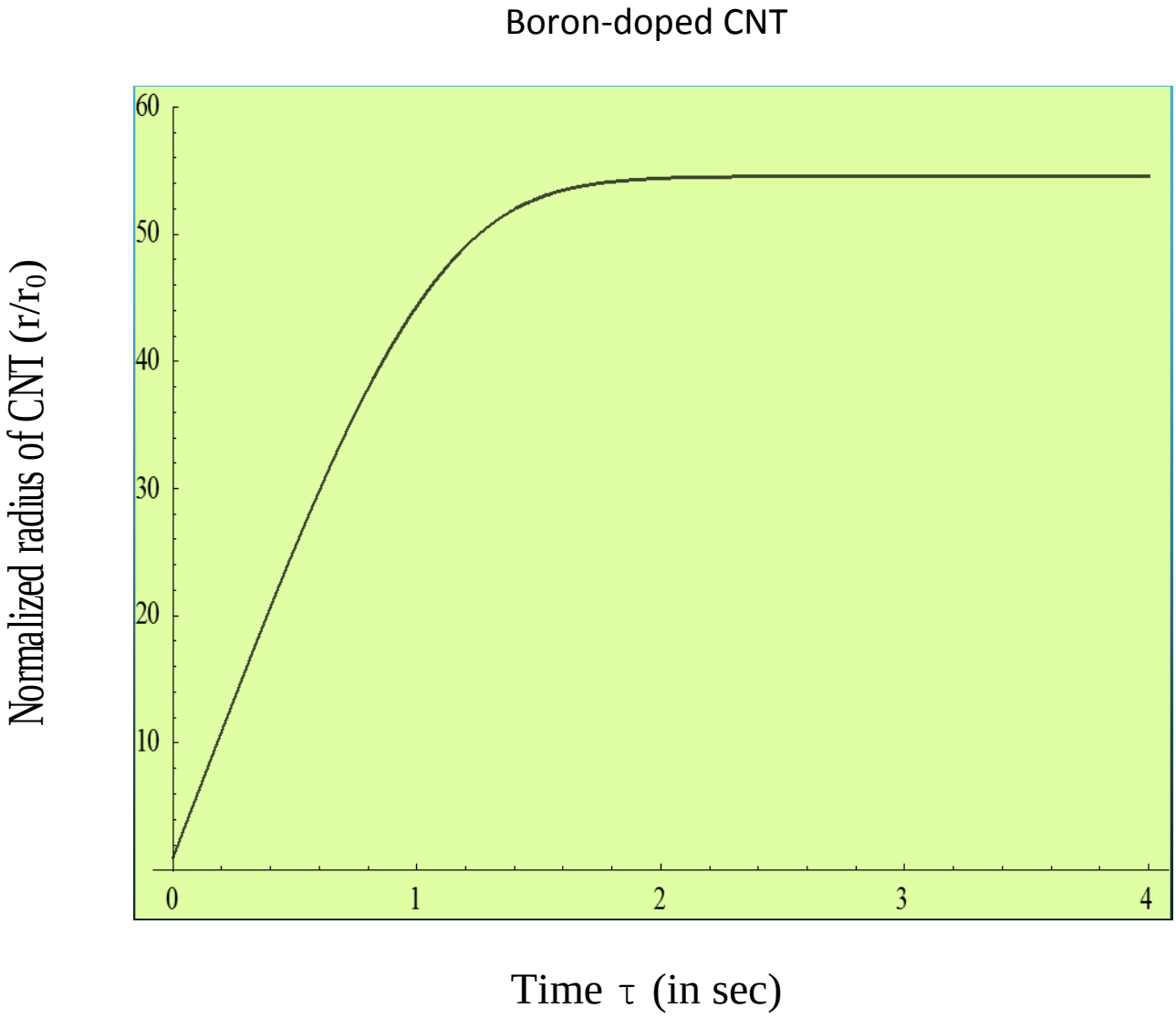

Fig3.5: Shows the variation of the normalized radius r/r_0 of spherical CNT tip placed over cylindrical surface for doped Boron using the parameters as (n_{ct}=10^6 cm^{-3} , $n_{iA0} = n_{iB0} = n_{iC0} = 10^7$ cm^{-3}, $n_{A0} = n_{B0} = n_{C0} = 10^{10}$ cm^{-3}, $n_{e0} = 10^7$ cm^{-3}, $T_{e0} = 1.3$eV, $T_{i0} = 2400$ K , $T_{n0} = T_{ct} = 1950$ K).

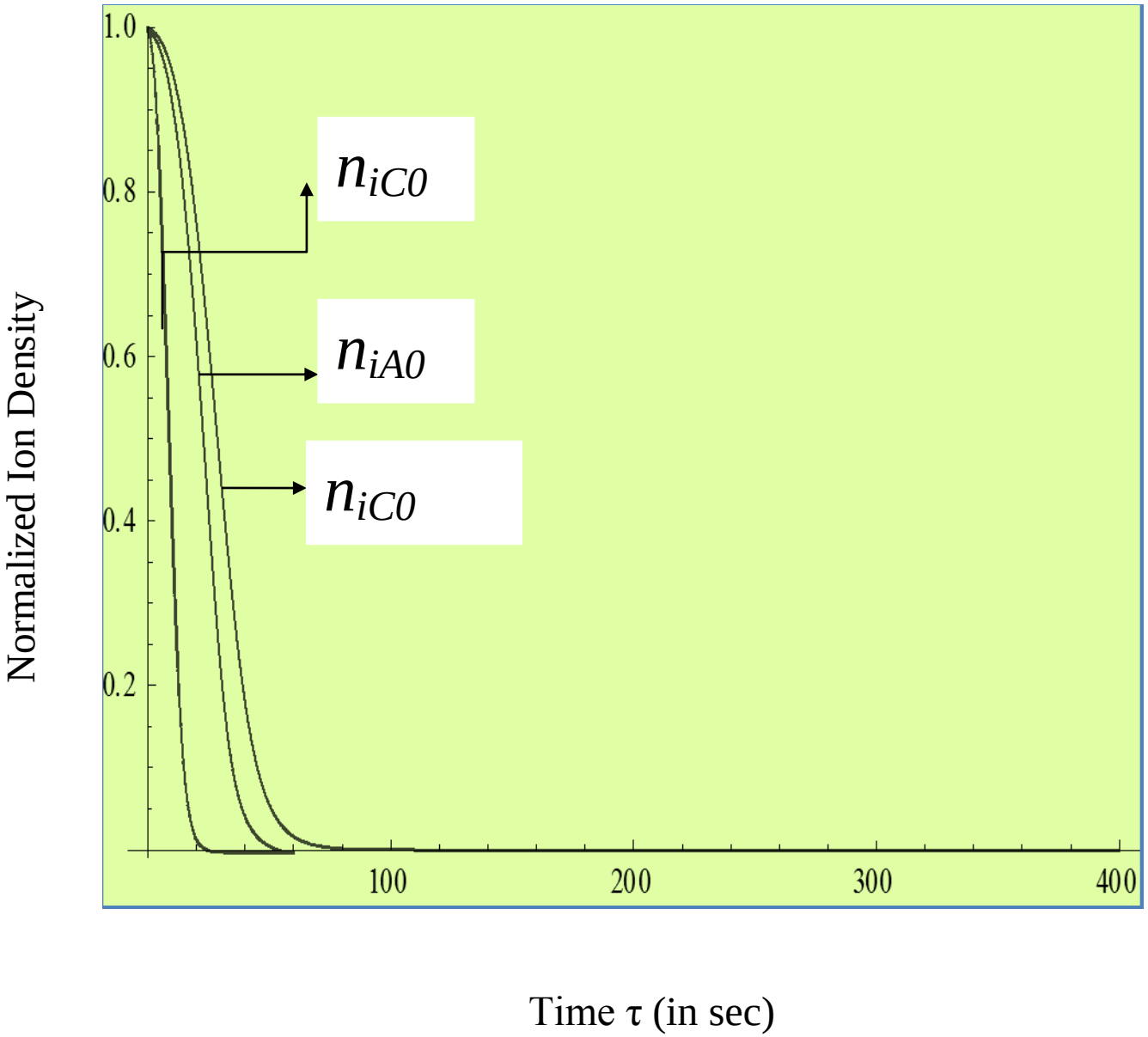

Fig.3.6: Shows the variation of normalized ion density for Carbon un-doped CNT (n_{iA0}), Nitrogen doped CNT (n_{iC0}), Boron doped CNT(n_{iC0}).The parameters taken are (n_{e0} =10^8 cm^{-3} and T_{e0}=0.5eV, n_{e0} =10^9 cm^{-3} and T_{e0}=1.5eV, n_{e0} =10^7 cm^{-3} and T_{e0}=1.3eV respectively).

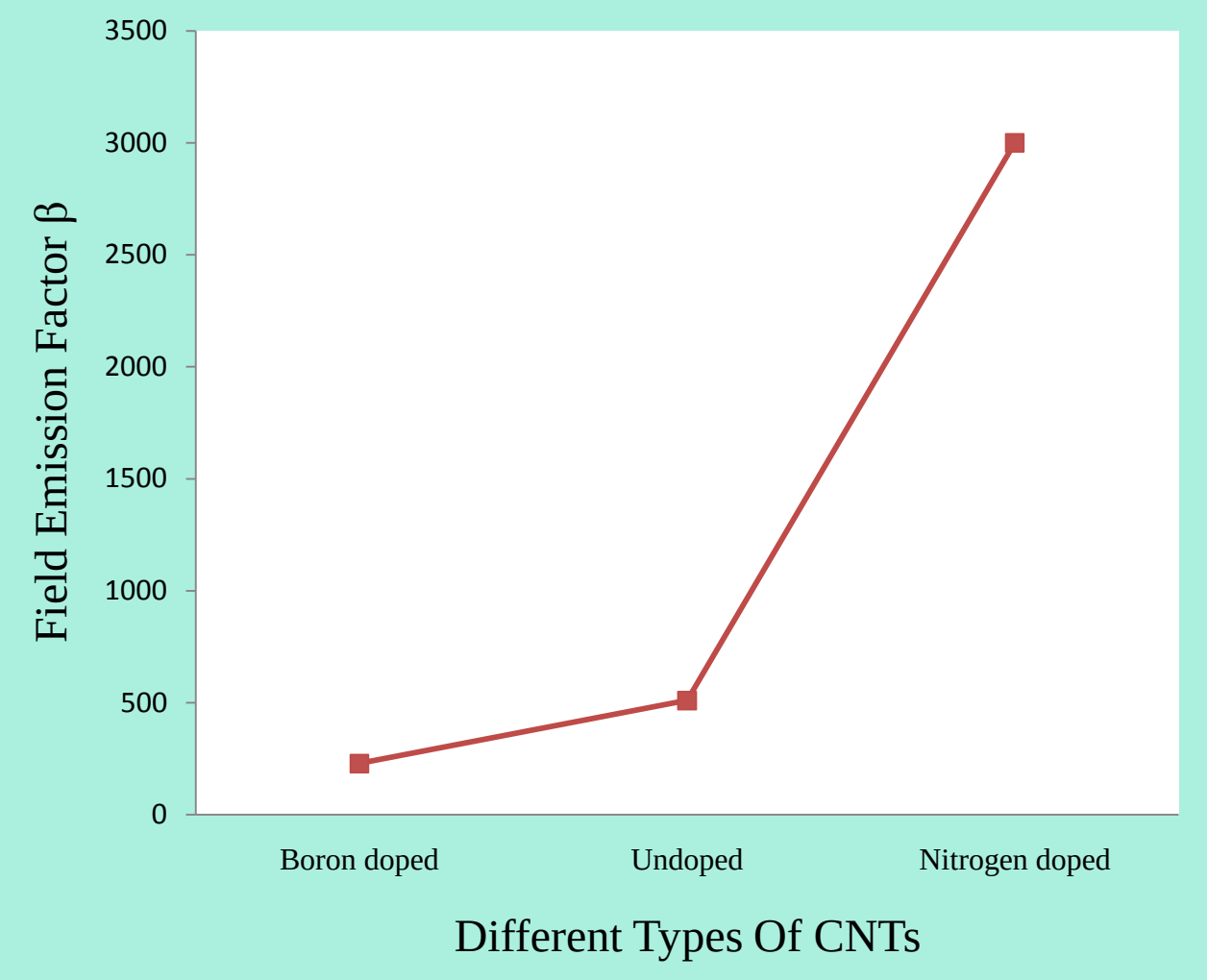

Fig.3.7: Shows the field emission factor for different types of CNTs, i.e, for Undoped CNT,N-doped CNT, B-doped CNT.

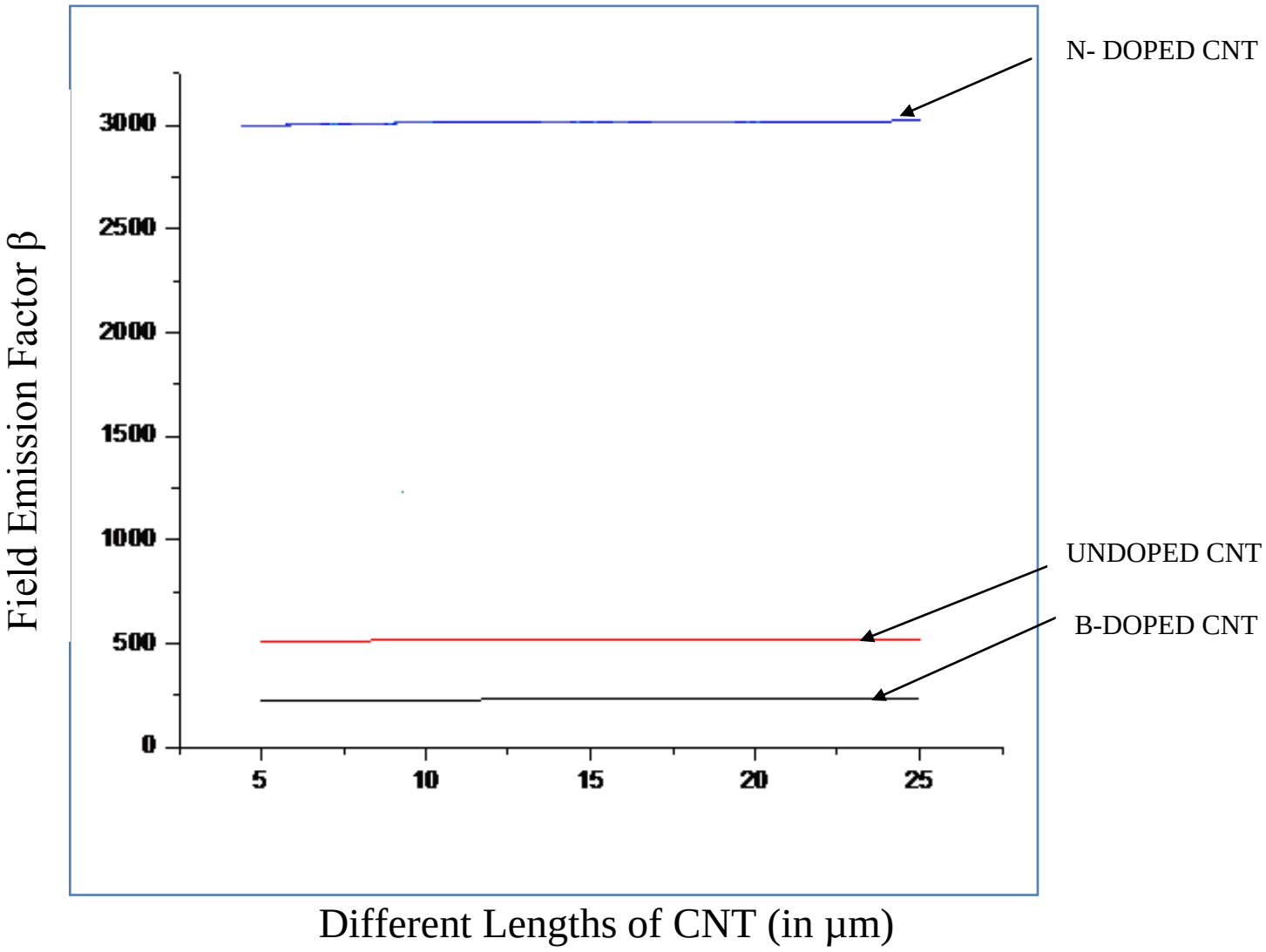

Fig.3.8: Shows the variation of field emission factor β with respect to different lengths of CNT for all three cases i.e. Undoped CNT, Boron doped CNT and Nitrogen doped CNT.

3.4 CONCLUSIONS

A theoretical model has been developed for calculating the radius of spherical CNT tip placed over the cylindrical surface with Nitrogen and Boron as doping elements. The effect of addition of these hetero-atoms has been calculated and analyzed with the help of an analytical model. The model includes the charging of CNT, charge neutrality, growth of electron density, neutral atom & positive ions density and energy balance of CNT with N & B as doping elements. It can be seen that doping of CNT with hetero atoms such as Nitrogen decreases the radius of CNT and Boron addition to CNT lattice increases its radius. We have also observed from our results that the length of CNT has little effect on the field emission properties of CNT while the radius of CNT plays an important factor in influencing the field emission property of CNT. Hence we conclude that with Nitrogen as doping material, the radius is tremendously reduced thereby increasing the field emission factor β manifolds with respect to Undoped and Boron doped CNTs.

REFERENCES

[1] D.H. Robertson, D.W. Brenner, J.W. Mintmire, Phys. Rev. B 45 (1992)12592.

[2] M.M.J. Treacy, T.W. Ebbesen, andJ.M. Gilson,Nature (London) 381 (1996) 678.

[3] E.W. Wong, P.E. Sheehan, C.M. Lieber, Science 277 (1997) 1971.

[4] M.F. Yu, O. Lourie, M.J. Dyer, K. Moloni, T.F. Kelly, R.S. Ruoff, Science 287 (2000) 637.

[5] J.P. Lu, Phys. Rev. Lett. 79 (1997) 1297.

[6] B.I. Yakobson, C.J. Brabec, J. Bernholc, Phys.Rev. Lett. 76 (1996) 2511.

[7] C.F. Cornwall, L.T. Wille, Solid State Commun. 101 (1997) 555.

[8] E. Herna´ndez, C. Goze, P. Bernier, A. Rubio, Phys. Rev.Lett. 80 (1998) 4502.

[9] V.N. Popov, V.E. Van Doren, M. Balkanski, Phys. Rev. B 61 (2000) 3078.

[10] D. Sa´nchez-Portal, E. Artacho, J.M. Soler, A. Rubio, Phys. Rev. B 59 (1999) 12678.

[11] S. Iijima, Helical microtubules of graphitic carbon, Nature (London) 354 (1991) 56.

[12] S. Iijima, T. Ichihashi, Nature (London) 363 (1993) 603.

[13] D.S. Bethune, C.H. Kiang, M.S. de Vries, G. Gorman, R. Savoy, J. Vazquez, R. Beyers, Nature (London) 363 (1993) 605.

[14] A. Thess, R. Lee, P. Nikolaev, H. Dai, P. Petit, J. Robert, C. Xu, Y.H. Lee, S.G. Kim, A.G. Rinzler, D.T. Colbert, G.E. Scuseria, D. Tomane´k, J.E. Fischer, R.E. Smalley, Science 273
(1996) 483.

[15] M.J. Yacaman, M.M. Yoshida, L. Rendon, J.G. Santiesteban, Appl. Phys. Lett. 62 (1993) 202.

[16]T. Guo, P. Nikolaev, A. Thess, D. T. Colbert and R. E. Smalley, Chem. Phys. Lett.,243,(1995)49-54.

[17] T. Ikegami, F. Nakanishi, M. Uchiyama and K. Ebihara,Thin Solid, (2004), 457, 7–11.

[18] A. P. Bolshakov, S. A. Uglov, A. V. Saveliev, V. I. Konov,A. A. Gorbunov, W. Pompe and A. Graff, Diamond Relat. Mater.,(2002), 11, 927–930.

[19] H. Y. Zhang, Y. Ding, C. Y. Wu, Y. M. Chen, Y. J. Zhu, Y. Y. He and S. Zhong, Phys. B (Amsterdam, Neth.), (2003), 325, 224–229.

[20] R. Marchiori, W. F. Braga, M. B. H. Mantelli and A. Lago, J. Mater. Sci., (2010), 45, 1495–1502.

[21] S. A. Steiner, T. F. Baumann, B. C. Bayer, R. Blume, M. A. Worsley, W. J. MoberlyChan, E. L. Shaw, R. Schlogl, A. J. Hart, S. Hofmann and B. L. Wardle, J. Am. Chem. Soc., (2009), 131, 12144–12154.

[22] H. Tempel, R. Joshi and J. J. Schneider, Mater. Chem. Phys., (2010),121, 178–183.

[23] R. Smajda, J. C. Andresen, M. Duchamp, R. Meunier, S. Casimirius, K. Hernadi, L. Forro and A. Magrez, Phys. Status Solidi B, (2009), 246, 2457–2460.

[24] S. P. Patole, P. S. Alegaonkar, H. C. Lee and J. B. Yoo, Carbon, (2008), 46, 1987–1993.

[25] H. R. Byon, H. Lim, H. J. Song and H. C. Choi,Bull. Korean Chem.Soc., (2007), 28, 2056–2060.

[26] Y. M. Chen and H. Y. Zhang, in Advances in Composites, ed. J. L.Bu, Z. Y. Jiang and S. Jiao, Trans Tech Publications Ltd, Stafa-Zurich, (2011), Pts 1 and 2, pp. 1560–1563.

[27] D. Varshney, B. R. Weiner and G. Morell, Carbon, (2010), 48, 3353–3358.

[28] H. D. Kim, J. H. Lee and W. S. Choi, J. Korean Phys. Soc., (2011), 58,112–115.

[29] B. Brown, C. B. Parker, B. R. Stoner and J. T. Glass, Carbon, (2011),49, 266–274.

[30]Y. Xu, E. Dervishi, A. R. Biris and A. S. Biris, Mater. Lett., (2011), 65,1878–1881.

[31] Y. J. Zhu, T. J. Lin, Q. X. Liu, Y. L. Chen, G. F. Zhang, H. F. Xiong and H. Y. Zhang, Mater. Sci. Eng., B, (2006), 127, 198–202.

[32] S. C. Lyu, B. C. Liu, C. J. Lee, H. K. Kang, C. W. Yang and C. Y. Park, Chem. Mater., (2003), 15, 3951–3954.

[33]R. Loffler, M.Haffner , G.Visanescu, H. Weigand ,X. Wang ,D. Zhang, M. Fleischer , A.J. Meixner, J. Fortagh, D.P. Kern, Carbon **49,** (2011)4197.

[34] S.C. Sharma and A. Tewari , Phys. Plasmas **18,** (2011)06503

[35]Sung Yool Choi, Young Kang and Kyoung Ik Cho, Journal of the Korean Physical Society **39**, (2001), 193.

[36]Se-Jin Kyung, Maksym Voronko, June-Hee Lee and Geun-Young Yeomet, Journal of the Korean Physical Society **47**, (2005) 824.

[37]Y.Y. Wang, S. Gupta, J.M. Garguilo, Z.J. Liu, L.C. Qin, R.J. Nemanich, Diamond & Related Materials **14**, (2005) 714.

[38]Shan-Sheng Yu, Wei-Tao Zheng, Nanoscale **2**, (2010) 1069.

[39]Jean-Marc Bonard , Hannes Kind, Thomas Stockili, Lars-Ola Nilsson,Solid State electronics **2586,** 1(2001).

[40]X.Q .Wang, M.Wang, P.M. He and Y.B. Xu, J. Appl. Phys. **96**, 6752 (2004).

[41] W. A. de Heer, A. Châtelain, D. Ugarte, Science **270**, 1179 (1995).

[42] Yu. V. Gulyaev, I. S. Nefedov, N. I. Sinitsyn, G. V. Torgashov, Yu. F. Zakharchenko, and A. I. Zhbanov, J. Vac. Sci. Technol. B **13**, 593 (1995).

[43] Y. Cheng, and O. Zhou, C. R. Physique **4**, 1021 (2003).

[44] J. Zhang, C. Yang, W. Yang, T. Feng, X. Wang, and X. Liu, Solid State Commun. **138**,13 (2006).

[45] J. M. Bonard, J. P. Salvetat, T. Stöckli, L. Forró, A. Châtelain, Appl. Phys. A **69**, 245 (1999).

[46] J. Robertson, Materials Today **7**, 46 (2004).

[47] R. Saini, Z. Jandric, M. Nolan, and S. A. M Mentink, *19th IEEE International Conference on Micro Electro Mechanical Systems, MEMS* (Istanbul), 918 (2006).

[48] S. Iijima. Nature (London) **354**, 56 (1991).

[49] H. Dai, Surf. Sci. **500**, 218 (2002).

[50]Duesberg GS, Graham A, Kreupl A, Liebau M, Seidel M, Unger E, et al.Diam Rel Mat 2006;13:354–61.

[51] Dresselhaus M, Dresselhaus G, Avouris P., Germany: Springer-Verlag; 2001.

[52] Tsang J, Freitag M, Perebeinos V, Liu J, Avouris P,Nature Nanotech 2007;2:725–30.

[53] Dresselhaus MS, Dresselhaus G,. Adv in Phys 1981;30:139–326.

[54] Stephan O, Ajayan P., Science 1994;266:1863–5.

[55] Xuefei Li ,Lingnan Kong ,Jinghai Yang,Ming Gao Appl Phys A (2013)113:735-739.[56]Antal A. Koos., Frank Dillon , E. A. Obraztsova , Alison Crossley ,
Nicole Grobert., Carbon **48,** 3033 (2010).

[57]Balaji Padya , Dipankar Kalita, P.K. Jain, G.Padmanabham, M.Ravi, K.S. Bhat , Appl. Nanosci. **2**,253 (2012).

[58]Sanjay K. Srivastava, V.D. Vankar, DV Sridhar Rao, V Kumar, Thin Solid Films **515** ,1851(2006).

[59]M. S. Sodha, Shikha Misra, S. K. Mishra and Sweta Srivastava , J. Appl.Phys.**107**, 103307 (2010).

[60]M. S. Sodha, S. K. Mishra and Shikha Misra, Phys. Plasmas **16**, 23701(2009).

[61]A. Tewari and S. C. Sharma ,J. Plasma Physics **79**, 939(2013).

[62]G. Zhang, W. Duan, and B. Gu, Appl. Phys. Lett. **80**, 2589(2002).

[63]Wen K. Hsu, Steven Firth, Philipp Redlich, Mauricio Terrones, Humberto Terrones , Yan Q. Zhu, Nicole Grobert , Andreas Schilder , Robin J.H Clark, Harold W. Kroto and David R.M. Walton, J. Mater. Chem. **10**, 1425(2000).

[64]S. F. Lee, Yung-Ping Chang, Li-Ying Lee, J. Mater. Sci. Mater. Electron **20**, 851(2009).

[65]S. K. Srivastava, A.K. Shukla, V. D. Vankar, and V. Kumar, Thin Solid Films **492**, 124(2005).

[66]Zhi Xu, X. D. Bai and E. G. Wang, Appl.Phys.Lett.**88**, 133107(2006).

[67]L.H. Chan, K. H. Hong and D. Q. Xiao W. J. Hsieh, S. H. Lai, H. C. Shih, T. C. Lin, F. S. Shieu, K. J. Chen and H. C. Cheng , Appl. Phys. Lett.**82**, 4334 (2003).

[68]G. Zhang, W. Duan, and B. Gu, Appl. Phys. Lett. **80**, 2589(2002).